FOCUSED FEASIBILITY STUDY REPORT
FOR
40TH AVENUE PROJECT AREA
IN THE ST. LOUIS RIVER AREA OF CONCERN

August 28, 2015

APPENDIX O. SUBMERGED AQUATIC AND FLOATING LEAF VEGETATION MODEL

Current Condtions 40th Ave. W

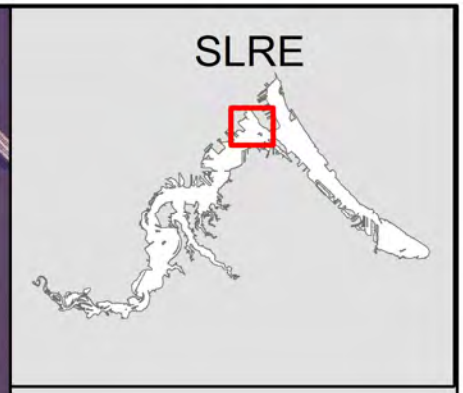

Legend

- FLV
- SAV

Data Sources: NAIP imagery, USEPA MED Lab

N

0 0.0750.15 0.3 Kilometers

Cartographer:Jonathon Launspach
EPA Contractor (SRA International)

40th Ave W
Aquatic Veg Output
for Islands
Current conditions:
FLV (floating leaf) = 11.713 ac
SAV (includes emergent and submergent) = 51.867 ac
Design with Shoals:
FLV (floating leaf) = 11.836 ac
SAV (includes emergent and submergent) = 85.869 ac
Legend
Floating leaf probability
0 - 0.6
0.6 - 1
SAV probability
0 - 0.75
0.75 - 1
N
0 0.05 0.1 0.2 0.3 0.4
Miles

40th Ave W
Aquatic Veg Output
for Islands
Current conditions:
FLV (floating leaf) = 11.713 ac
SAV (includes emergent and submergent) = 51.867 ac
Design with Islands:
FLV (floating leaf) = 14.851 ac
SAV (includes emergent and submergent) = 72.501 ac
Legend
Floating leaf probability
0 - 0.6
0.6 - 1
SAV proability
0 - 0.75
0.75 - 1
N
0 0.05 0.1 0.2 0.3 0.4
Miles

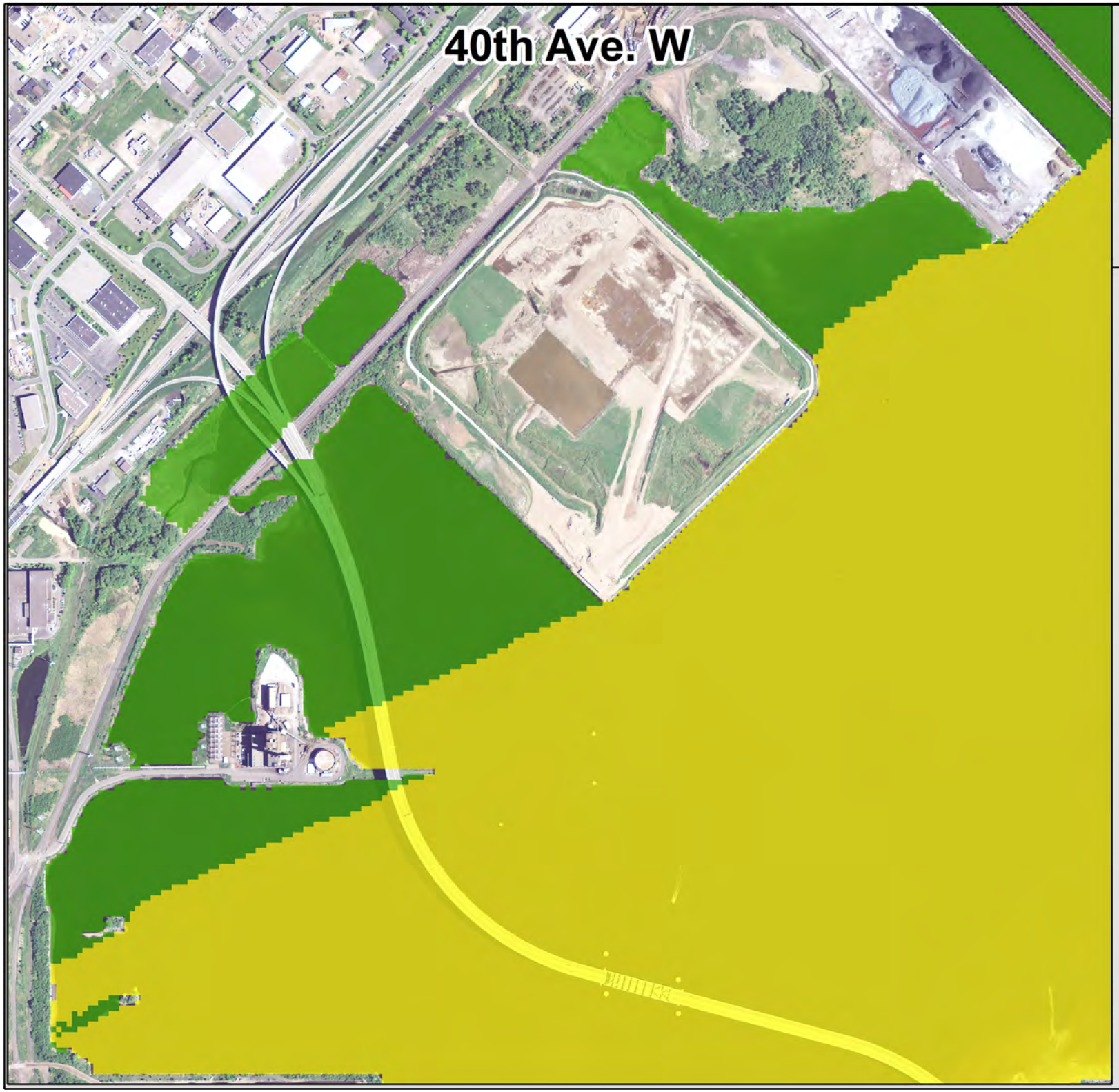

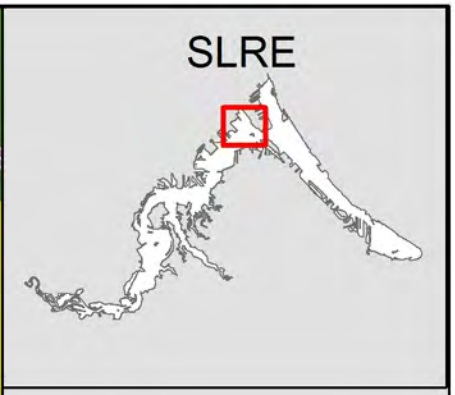

Legend

REI

71 - 4,000

4,000- 13,470

Data Sources: NAIP imagery, USEPA MED Lab

N

0 0.050.1 0.2 Kilometers

Cartographer:Jonathon Launspach
EPA Contractor (SRA International)

For: Joe Kreitinger USACE

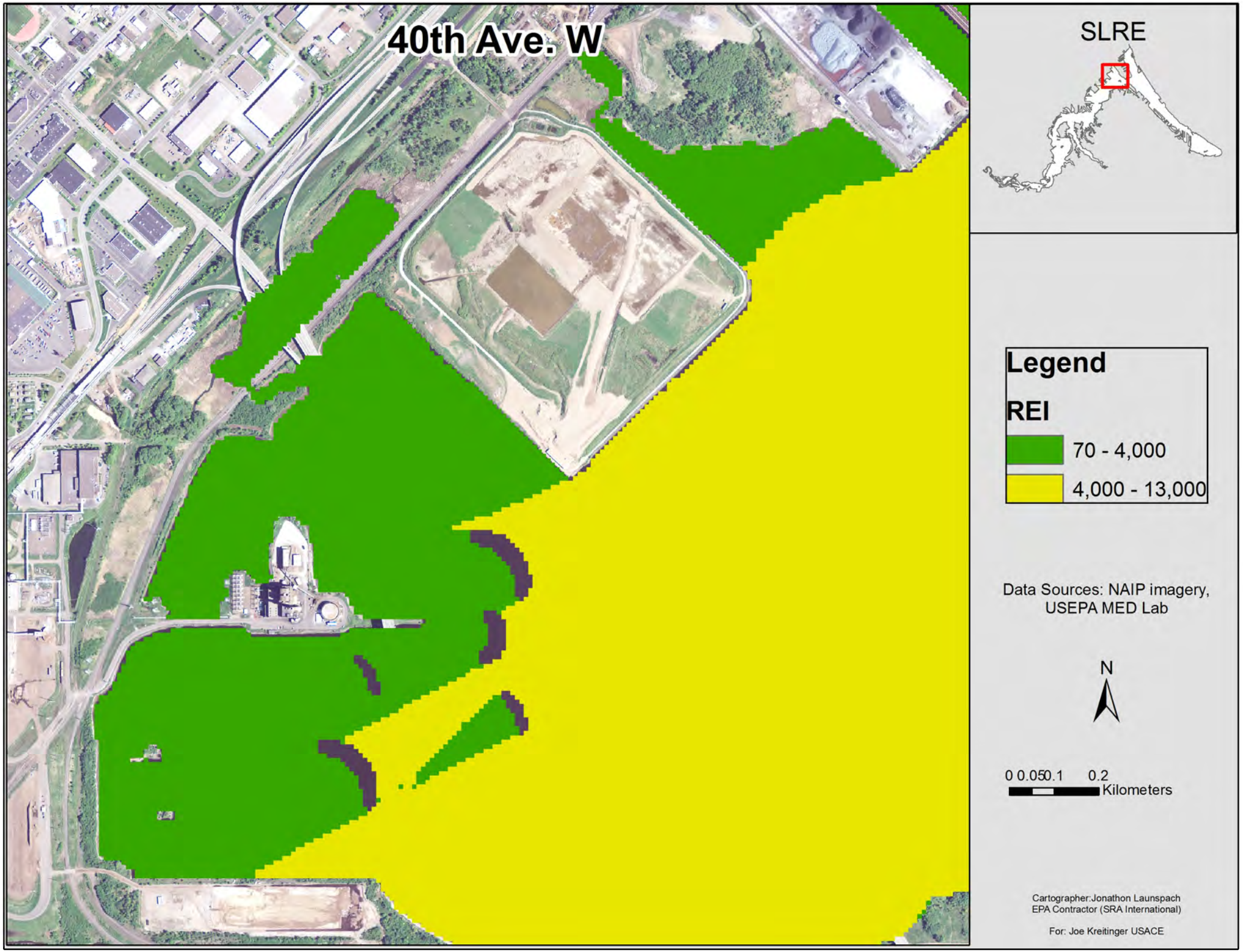
40th Ave. W
SLRE
Legend
REI
70 - 4,000
4,000 - 13,000
Data Sources: NAIP imagery, USEPA MED Lab
N
0 0.050.1 0.2
Kilometers
Cartographer:Jonathon Launspach
EPA Contractor (SRA International)
For: Joe Kreitinger USACE

Chart for determing depth and REI combinations favoring SAV in St. Louis Bay of the St. Louis River
Based on models in Angradi et al. 2013, JGLR 39:539-549
Chart most reliable for depth ≥ 0.5m and REI ≤ 14000

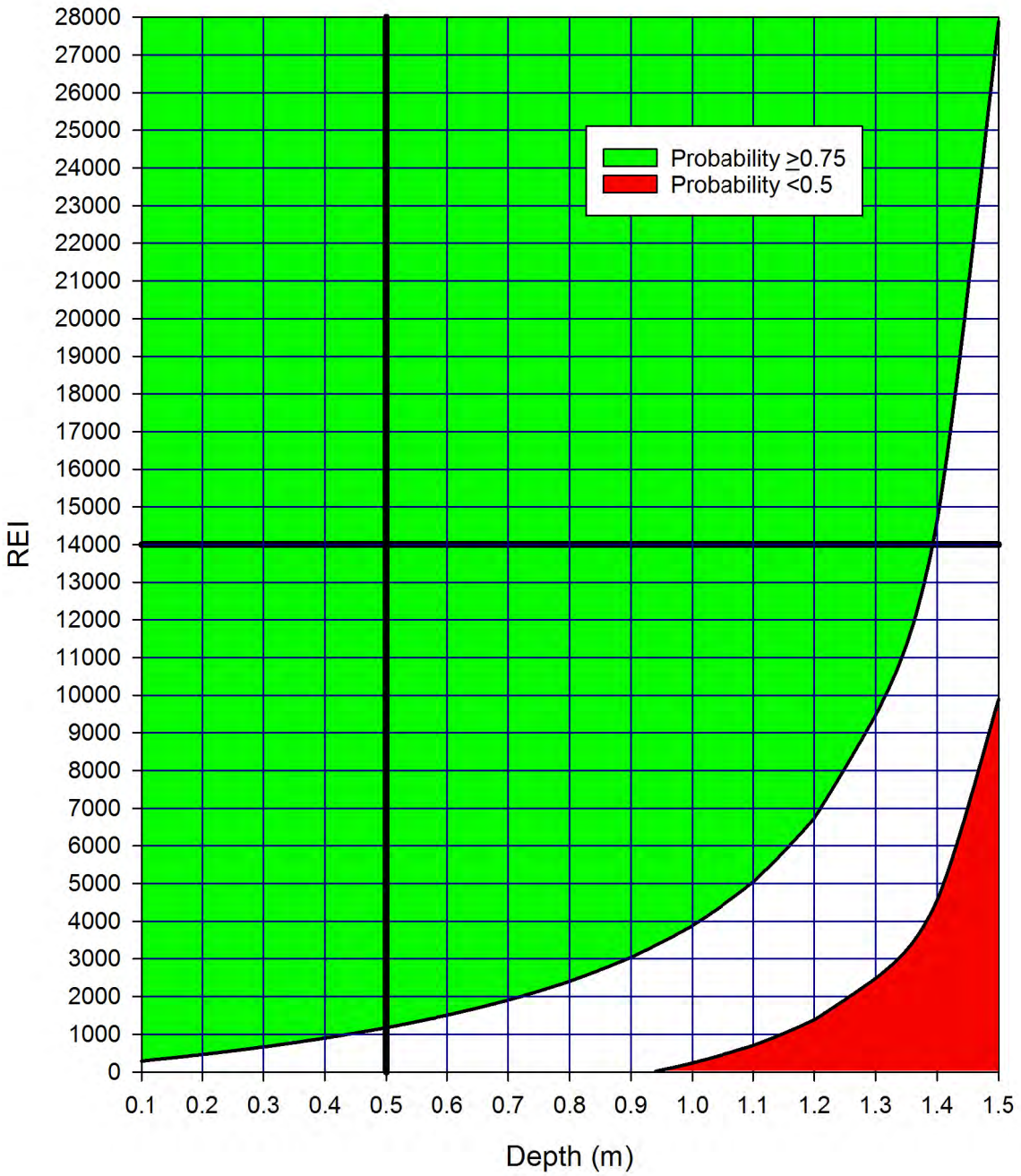

A predictive model for floating leaf vegetation in the St. Louis River Estuary

Prepared for

Minnesota Pollution Control Agency
Duluth, MN

Prepared by

United States Environmental Protection Agency
Office of Research and Development
National Health and Environmental Effects Research Laboratory
Mid-Continent Ecology Division
Duluth, MN
Contact: Ted Angradi; angradi.theodore@epa.gov

Background

In summer 2014, USEPA staff was asked by MPCA to develop a predictive model for floating leaf vegetation (FLV) in the St. Louis River Estuary (SLRE). The existing model (Host et al. 2012) greatly overpredicts FLV in St. Louis Bay probably because it was based on a limited number of observations of this wetland type and because their definition of FLV included areas of mixed floating and submerged aquatic vegetation, which is more widespread than true FLV. A more reliable model specific to floating plants could be included in the biological design basis for restoration projects in the SLRE.

Objective

Our objective was to create a predictive logistic mode to predict probability of occurrence of FLV in the SLRE. Previous wetland vegetation models for the SLRE (Angradi et al. 2013, Host et al. 2012) were based on visual or hydroacoustic detection of FLV. The model described herein was developed from data derived from photo-interpretation.

Methods

Preliminary analysis of Google Earth (GE) Imagery for August 2010 strongly suggested that certain species of FLV could be detected in the images. Field visits showed that many "stands" of white (*Nymphaea*) and yellow (*Nuphar*) water lilies could be reliably discerned from canopy-forming submerged aquatic vegetation and other vegetation types.

We created 5000 random points for the SLRE between the Blatnik and Oliver bridges, Using the polygon tool in GE, we circled 456 points where FLV (lily pads) was present under, surrounding or immediately adjacent to the point (Figure 1). We circled 698 points where the grid was either

in error because the points was on land or the point was in a pure stand of emergent vegetation (not mixed with FLV). The remaining 3816 points were designated as FLV absent.

In GIS, we extracted the depth, REI and weighted fetch for all of points where FLV was present or absent. Using logistic modeling methods similar to those described in Angradi et al. 2013, we created a logistic model to fit the data. The dependent variable was FLV present (1) or absent (0). Candidate predictor variables were depth, depth^2, Relative Exposure Index (REI), REI^2, and depth * REI.

The resulting models coefficients can be used to calculate the probability of FLV for any combination of depth (m) and REI. Note that predictions (yhat) in log odds must be converted to probabilities using the equation: probability of FLV (0-1) = $e^{yhat}/ (1+e^{yhat})$.

Results

Most FLV was at a depth of 0.2 to 1.3 m (the 10th and 90th percentiles of observed depths) (Figure 2). Likewise, nearly all FLW was at an REI between 640 and 2800. FLV was often absent present at points with depth and REI conditions otherwise favorable for FLV. The range of depth and exposure of conditions where FLV was present were a small subset of the total depth and REI range for the SLRE between the Blatnik and Oliver bridges (Figure 2)

The Appendix shows the regression results for the logistic model to predict probability of FLV. All parameters except REI were included in the final model (but REI^2 was included). Nagelkerke's adjusted coefficient of determination was 0.51. Concordance was 93%.

A model simulation (Figure 3A) shows the probability of FLV was highest (≈0.64) at a depth of 0.6– 0.7 m for all degrees of exposure (REI). Probability of FLV was highest (>0.5) at an REI of 800–1200 for all depths between 0.4 and 1 m. The simulation (and underlying model given in the Appendix), and Table 1 can be used to find combinations of depth and REI that are likely to result in the eventual establishment of FLV stands that include *Nymphaea* and *Nuphar* in the SLRE.

Assuming a cutoff probability of 0.6 or 60%, depth must be 0.4–0.9 m and REI must be <1700 for FLV to occur (Figure 4B; weighted fetch values can be derived from REI using the information in Figure 5). Assuming a cutoff probability of 50%, depth must be 0.2 –1.1 and REI must be <2500 for FLV to occur.

Figure 4B illustrates the interacting effect of depth and REI. The range of depths suitable for FLV depends on REI (e.g., the range narrows as REI exceeds 1000). Likewise, the range of REI suitable for FLV declines as depth exceeds 0.7 m. We speculate that in shallow, low exposure conditions, FLV may be outcompeted by (or mixed with) emergent vegetation. The reason why

FLV is predicted to be more likely at relatively deep locations of moderate exposure than at deep locations of low or high exposure is not clear.

The model appears to do an excellent job predicting FLV where it actually occurs upriver of Grassy Point (Figure 5). In lower St. Louis Bay, however, the model predicts the occurrence of FLV in some areas where FLV was not present in the 2010 images (Figure 5, continuation). We consider three possible underlying reasons for this model error.

1. FLV is present but not visible in imagery.
2. The underlying depth or fetch data for the 10 m grid is wrong.
3. One or more important predictors are missing from the model.

We reject reason 1 because the model was build based water lilies, which were clearly absent from some areas where it is predicted by the model. Reason 2 may be important in some areas where true depth (in August 2010) was deeper than the available bathymetric data. Reason 3 may account for the overprediction of FLV in the northern part of St. Louis Bay (the 21st Avenue West project area). For example, the model predicts FLV at the mouth of Miller Creek and near the WLSSD outfall where no FLV was present. The model still outperforms the existing model (Host et al. 2012) for this area, which predicted large areas of FLV including around Interstate Island. The missing predictor may be substrate composition, which was a weak predictor in the Host (2012) model, water flow, or an anthropogenic stressor associated with the tributary or the outfall. High flows in Miller Creek may directly (disturbance) or indirectly (substrate particle size and contamination) account for the lack of FLV at the mouth of the tributary where REI and depth are otherwise suitable.

Conclusions

1. The predictive model described herein is based on more points than the model of Host et al. 2012 and is more accurate (predictions compares better with actual FLV stands).
2. There is a strong interaction between exposure and depth that determines the physical conditions where FLV can occur in the SLRE.
3. The predicted REI limit for high probability FLV occurrence was ≈1700. The predicted depth limit for FLV occurrence was ≈ 0.9 m.
4. The model is applicable from Blatnik to Oliver Bridge, but may overpredict FLV in north St. Louis Bay for reasons that are not clear.

References

Angradi, Ted R., et al. "Predicting submerged aquatic vegetation cover and occurrence in a Lake Superior estuary." *Journal of Great Lakes Research* 39.4 (2013): 536-546.

Host, G., Reschke, C., Brady, V., Breneman, D., Dumke, J., Niemi, G., Austin, J., James, M., and Johnson, L. 2012. 21st Avenue West Remediation to Restoration Project: Biological Survey and Hydrodynamic Modeling. Natural Resources Research Institute, University of Minnesota, Duluth. Contracted by the United States Fish and Wildlife Service Cooperative Agreement F11AC00517.

Figure 1. Google earth images from near Clyde Avenue Landing showing polygons selecting random points where FLV was present. Some FLV is not visible at this zoom level.

Figure 2. Depth and REI characteristics at grid locations where FLV was present and absent. In the box plots, the dashed line is the mean, and symbols are the 5th and 95th percentiles.

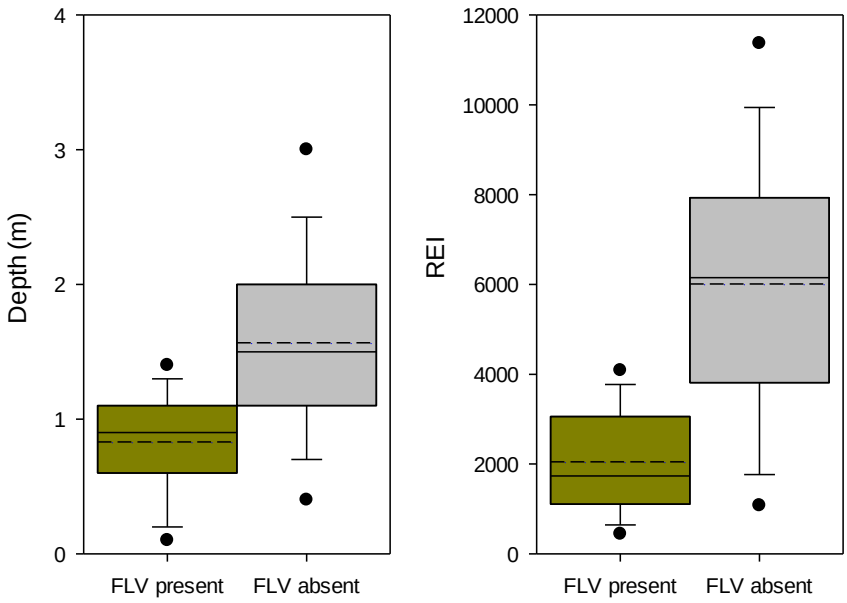

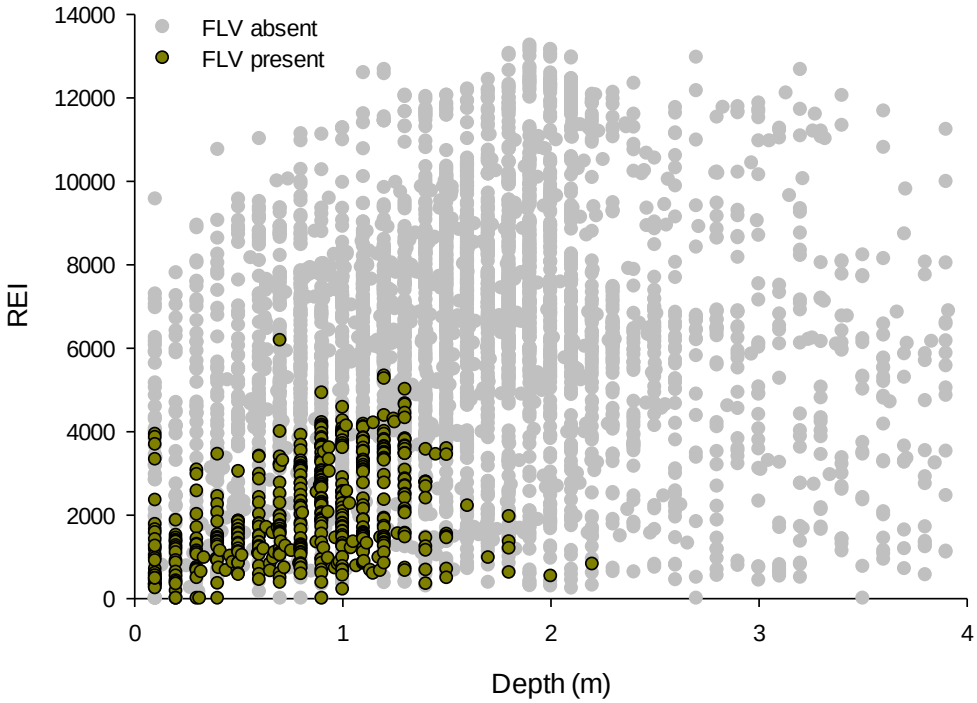

Figure 3. Model simulations for full logistic model (See Appendix). In plot A, curves show the effect of REI on probability of FLV for different depths. In plot B, the depth and REI are plotted for all 10 m grid locations between Blatnik Bridge and Oliver Bridge for which the predicted probability of FLV was ≥ 0.5 or 0.6.

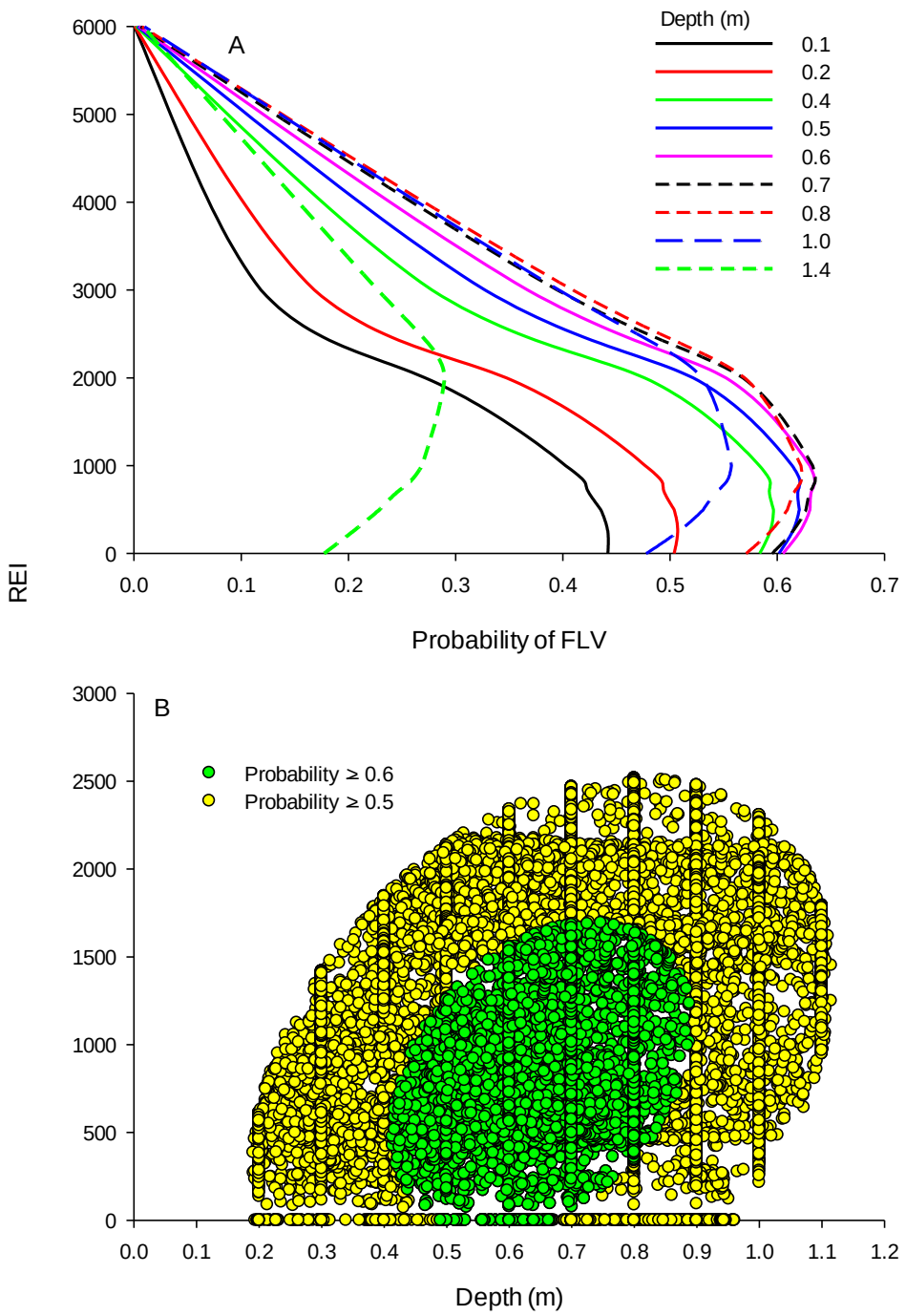

Figure 4. Empirical relationship for converting REI to weighted fetch. Points are locations with FLV.

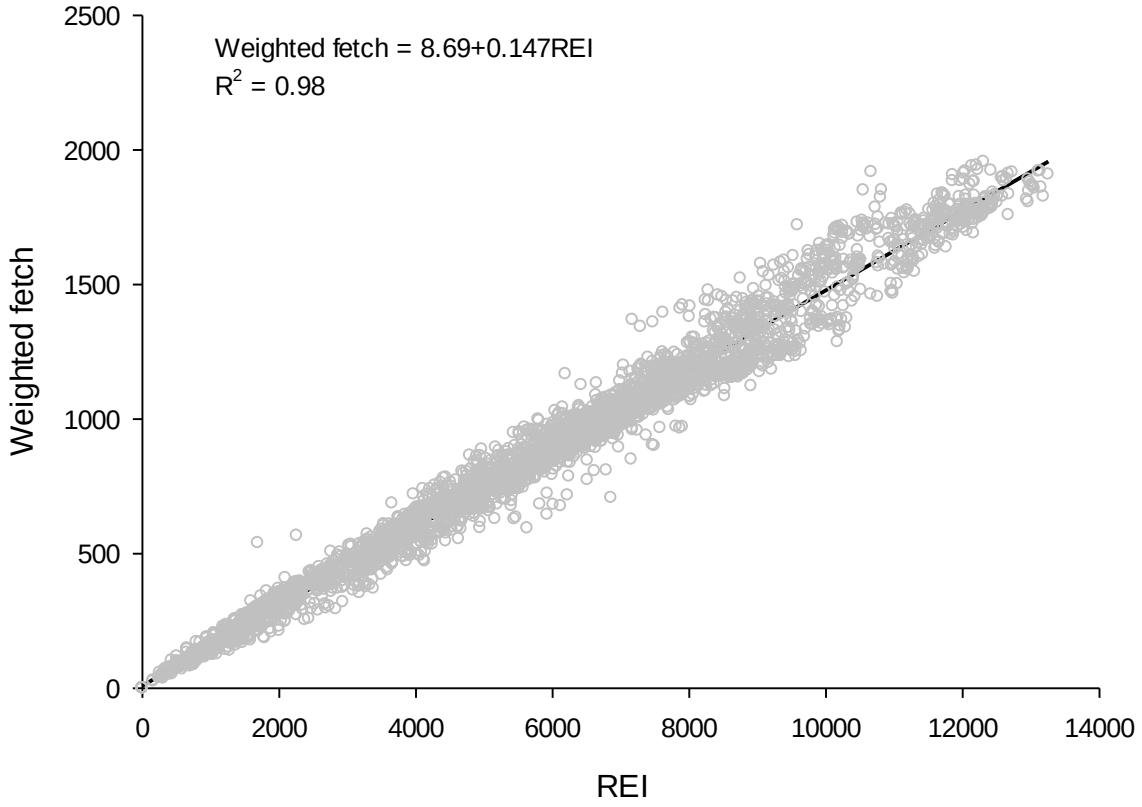

Figure 5. Model prediction of FLV occurrence (probability ≥0.6 and 0.5) in the SLRE.

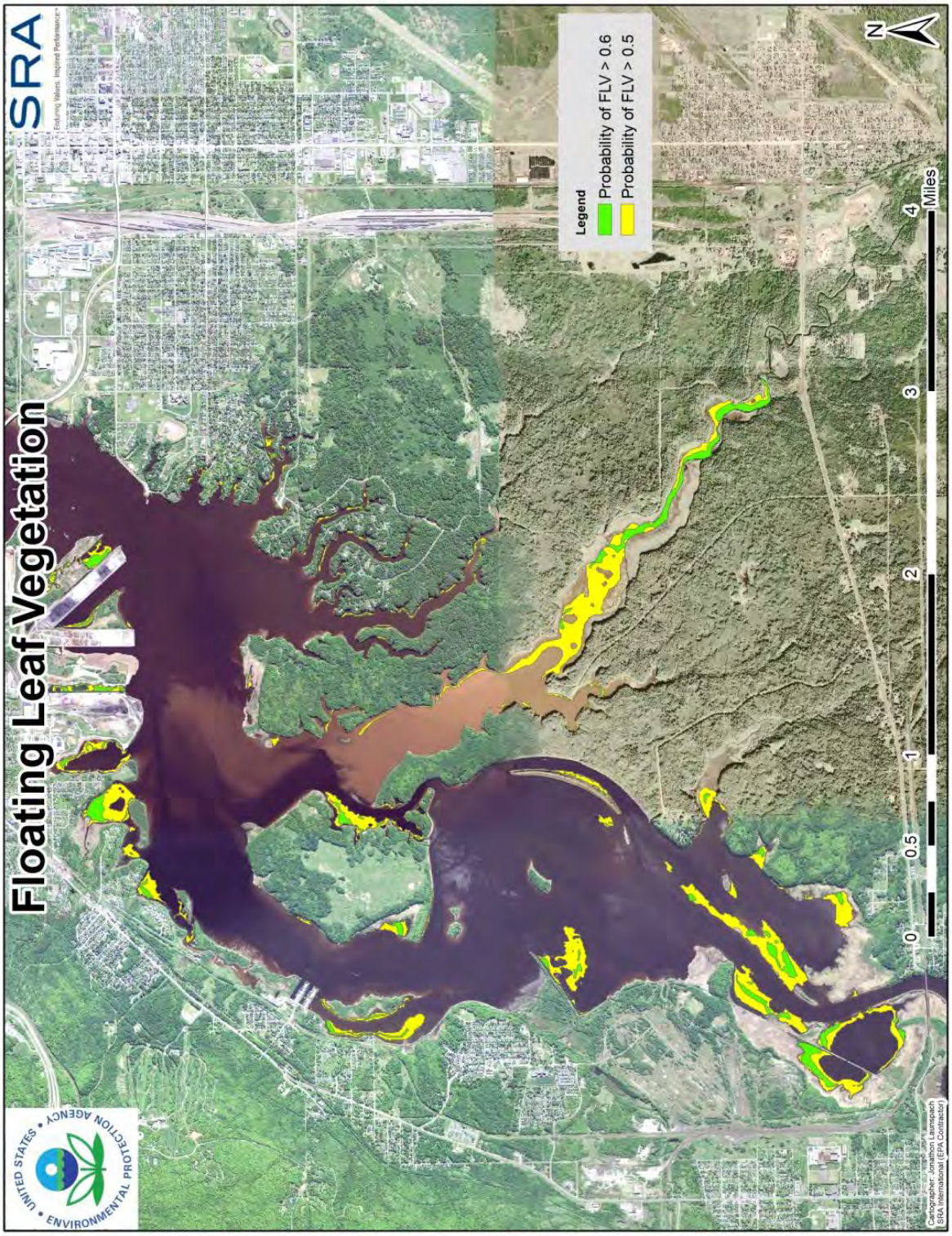

Figure 5. Continued.

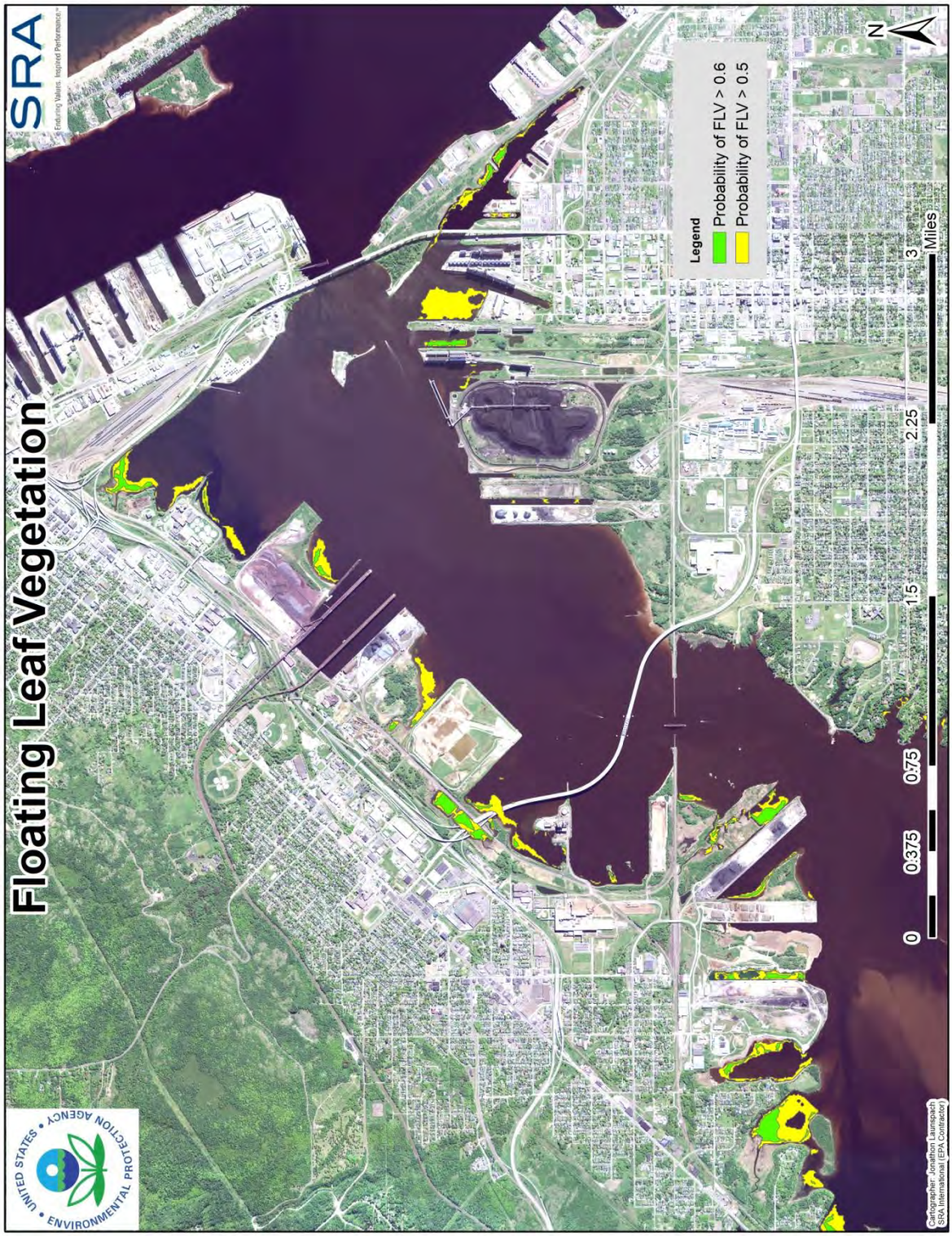

Table 1. Depth range by REI and REI range by depth for which the probability of FLV is maximized (probability $\geq$ 0.6).

Depth (m)	REI range	
	Minimum	maximum
0.40	400	600
0.45	100	1100
0.50	0	1300
0.55	0	1400
0.60	0	1600
0.65	0	1600
0.70	0	1700
0.75	0	1700
0.80	300	1700
0.85	500	1600
0.90	900	1300

REI	Depth range (m)	
	Minimum	Maximum
0	0.50	0.70
100	0.45	0.70
200	0.45	0.75
300	0.45	0.80
400	0.40	0.80
500	0.40	0.85
600	0.40	0.85
700	0.45	0.85
800	0.45	0.85
900	0.45	0.90
1000	0.45	0.90
1100	0.45	0.90
1200	0.50	0.90
1300	0.50	0.90
1400	0.55	0.85
1500	0.60	0.85
1600	0.60	0.85
1700	0.70	0.80

Appendix. SAS code (with model results) for logistic regression model

```
*file FLV1;
libname FLV 'M:\Biosonics data\lindgren rake survey';

***FLV random points model;
*5000 random points overlay on GE images;
*FLV Present or absent or land determined;

proc import out =flv.FLV5
datafile = 'M:\Biosonics data\lindgren rake
survey\5000randompoints8_25_14.csv'
dbms = csv replace;     getnames = yes; guessingrows = 2000; run;
*proc print data = flv.flv5 (obs = 1000);run;


*create new predictor variables;
data flv.flv6;set flv.flv5;
if covertype = -1 then delete;*grid error = land;
if covertype = 0 then flv_pa = 0;*FLV present;
if covertype = 2 then flv_pa =1;
if flv_pa = 1 and rei >7000 then delete;*outlier;
if flv_pa = 1 and depth <-3 then delete;*outlier;
depth = depth *-1;
Depth_sqr = depth *depth;
REI_sqr = REI * REI;
DEPTHxREI= depth * REI;
If depth lt 0.1 then depth = 0.1;*grid error;
run;


***full models;
**model selection;
proc logistic descending data = flv.flv6;
model flv_pa = depth rei depth_sqr rei_sqr depthxrei/  selection = stepwise
rsquare ; run;
*rei dropped;

**final full model;
proc logistic descending data = flv.flv6;
model flv_pa = depth depth_sqr rei_sqr depthxrei /  rsquare ;
output out=predFLV  p = yhat ; run;
```

```
*  MODEL results

                                The LOGISTIC Procedure

                                  Model Information

                     Data Set                      FLV.FLV6
                     Response Variable             flv_pa
                     Number of Response Levels     2
                     Model                         binary logit
                     Optimization Technique        Fisher's scoring


                        Number of Observations Read        4122
                        Number of Observations Used        4122


                                Response Profile

                           Ordered                      Total
                             Value       flv_pa     Frequency

                                 1            1           484
                                 2            0          3638

                            Probability modeled is flv_pa=1.


                                Model Convergence Status

                     Convergence criterion (GCONV=1E-8) satisfied.


                                Model Fit Statistics

                                                   Intercept
                                     Intercept            and
                         Criterion        Only     Covariates

                         AIC           2984.269       1687.795
                         SC            2990.593       1719.416
                         -2 Log L      2982.269       1677.795


                  R-Square    0.2713    Max-rescaled R-Square    0.5268
                  Nagelkerke R-square 0.51

                        Testing Global Null Hypothesis: BETA=0

                 Test                 Chi-Square       DF     Pr > ChiSq

                 Likelihood Ratio      1304.4736        4         <.0001
                 Score                  718.7658        4         <.0001
                 Wald                   325.7926        4         <.0001
```

```
                                The LOGISTIC Procedure

                        Analysis of Maximum Likelihood Estimates

                                              Standard      Wald
          Parameter    DF    Estimate        Error    Chi-Square    Pr>chisq

         Intercept     1     -0.5394       0.2279        5.6010        0.0180
         Depth         1      3.3541       0.5424       38.2400        <.0001
        Depth_sqr     1     -2.9041       0.2988       94.4848        <.0001
         REI_sqr       1    -2.15E-7     2.391E-8       80.9766        <.0001
         DEPTHxREI     1    0.000535     0.000126       18.0261        <.0001
                                Odds Ratio Estimates

                                   Point          95% Wald
                     Effect       Estimate      Confidence Limits

                     Depth          28.620       9.885      82.864
                     Depth_sqr       0.055       0.031       0.098
                     REI_sqr         1.000       1.000       1.000
                     DEPTHxREI       1.001       1.000       1.001

             Association of Predicted Probabilities and Observed Responses

                    Percent Concordant       92.4    Somers' D    0.850
                    Percent Discordant        7.4    Gamma        0.851
                    Percent Tied              0.2    Tau-a        0.176
                    Pairs                 1760792    c            0.925

end model results;


proc import out =grid
datafile = 'M:\Biosonics data\lindgren rake survey\grid.csv'
dbms = csv replace;     getnames = yes; guessingrows = 2000; run;
*Output predictions for plots;
data grid60 ;set grid;
depth = depth *-1;
Depth_sqr = depth *depth;
REI_sqr = REI * REI;
DEPTHxREI= depth * REI;
if depth <0.1 then delete;
*model;
yhattest = -0.5394 + (3.3541 * depth) + (-2.9041*depth_sqr) + (-2.15e-
7*rei_sqr)+ (0.000535*depthxrei);
*convert log odds to  prob;
probflv = exp(yhattest)/(1+(exp(yhattest)));
*toggle;
*if probflv Lt 0.5 then delete;
if probflv Lt 0.6 then delete;
run;
proc print data =grid60 (obs = 100);run;
proc export data = grid60
outfile= 'M:\Biosonics data\lindgren rake survey\flvgrid60_rand'
DBMS = excel replace;run;
***********end random flv models;
```

Journal of Great Lakes Research 39 (2013) 536–546

Contents lists available at ScienceDirect

Journal of Great Lakes Research

journal homepage: www.elsevier.com/locate/jglr

Predicting submerged aquatic vegetation cover and occurrence in a Lake Superior estuary

Ted R. Angradi [a,*], Mark S. Pearson [a], David W. Bolgrien [a], Brent J. Bellinger [a], Matthew A. Starry [b], Carol Reschke [c]

[a] U.S. Environmental Protection Agency, Office of Research and Development, National Health and Environmental Effects Research Laboratory, Mid-Continent Ecology Division, 6201 Congdon Blvd., Duluth, MN 55804, USA
[b] SRA International, Inc., 6201 Congdon Blvd., Duluth, MN 55804, USA
[c] University of Minnesota Duluth, Natural Resources Research Institute, 5013 Miller Trunk Hwy., Duluth, MN 55811, USA

ARTICLE INFO

Article history:
Received 8 August 2013
Accepted 16 September 2013
Available online 18 October 2013

Communicated by Lars Rudstam

Index words::
St. Louis River
Lake Superior
Hydroacoustic survey
Predictive model
Submerged aquatic vegetation
Ecosystem services

ABSTRACT

Submerged aquatic vegetation (SAV) provides the biophysical basis for multiple ecosystem services in Great Lakes estuaries. Understanding sources of variation in SAV is necessary for sustainable management of SAV habitat. From data collected using hydroacoustic survey methods, we created predictive models for SAV in the St. Louis River Estuary (SLRE) of western Lake Superior. The dominant SAV species in most areas of the estuary was American wild celery (*Vallisneria americana* Michx.). Maximum depth of SAV in 2011 was approximately 2.1 m. In regression tree models, most of the variation in SAV cover was explained by an autoregression (lag) term, depth, and a measure of exposure based on fetch. Logistic SAV occurrence models including water depth, exposure, bed slope, substrate fractal dimension, lag term, and interactions predicted the occurrence of SAV in three areas of the St. Louis River with 78–86% accuracy based on cross validation of a holdout dataset. Reduced models, excluding fractal dimension and the lag term, predicted SAV occurrence with 75–82% accuracy based on cross validation and with 68–85% accuracy for an independent SAV dataset collected using a different sampling method. In one area of the estuary, the probability of SAV occurrence was related to the interaction of depth and exposure. At more exposed sites, SAV was more likely to occur in shallow areas than at less exposed sites. Our predictive models show the range of depth, exposure, and bed slope favorable for SAV in the SLRE; information useful for planning shallow-water habitat restoration projects.

Published by Elsevier B.V. on behalf of International Association for Great Lakes Research.

Introduction

Submerged aquatic vegetation (SAV) provides the biophysical basis for multiple ecosystem services in aquatic ecosystems (Kahn and Kemp, 1985), including coastal systems in the Laurentian Great Lakes (Sierszen et al., 2012). SAV is a component of rearing and adult habitat for commercially and recreationally important Great Lakes sport fishes (Cvetkovic et al., 2010; Jude and Pappas, 1992; Randall et al., 1996). SAV beds provide habitat for invertebrates (Krieger, 1992) and forage for waterfowl (Knapton and Petrie, 1999; Prince et al., 1992). SAV also has an important role in ecosystem functions including nutrient cycling (Carpenter and Lodge, 1986; Wigand et al., 2000), wave attenuation (Christiansen et al., 1981; Koch, 2001), and sediment and water quality dynamics (Barko et al., 1991; Best et al., 2008; Madsen et al., 2001).

The St. Louis River Estuary (SLRE) is located within the St. Louis River "Area of Concern" (AOC; http://www.epa.gov/glnpo/aoc/stlouis/index.html; accessed 7 August 2013), an international designation recognizing that the system has experienced significant environmental degradation, and some ecosystem services or "beneficial uses" of the estuary have been lost or are degraded. In the SLRE AOC, beneficial use impairments include those that are related to SAV abundance and distribution. An example is the beneficial use impairment "loss of fish and wildlife habitat." SAV is a critical shallow-water habitat for fish and wildlife populations. In the SLRE, much of this habitat has been lost or degraded due to sediment contamination, wetland filling, and channel dredging. For this use impairment to be "delisted" for the AOC, shallow water and wetland habitat must be restored. Prior to restoration, it may be necessary to remediate sediments containing non-native material (e.g., wood waste, industrial debris) or sediments contaminated with metals and organic compounds. Following remediation and in areas of uncontaminated sediments, restoration of natural substrates and bathymetric contours to within limits favorable for SAV (and other wetland types) is a key restoration objective (SLRCAC, 2002).

Efficient SAV restoration planning requires reliable information about the physical habitat requirements that underlie the local distribution of native SAV species. The objective of this study was to examine factors accounting for variation in the distribution and abundance of

* Corresponding author. Tel.: +1 218 529 5243, +1 218 720 4338.
E-mail address: angradi.theodore@epa.gov (T.R. Angradi).

0380-1330/$ – see front matter. Published by Elsevier B.V. on behalf of International Association for Great Lakes Research.
http://dx.doi.org/10.1016/j.jglr.2013.09.013

SAV in the SLRE within the context of spatially explicit predictive models. These models can inform restoration efforts and conservation in the SLRE and elsewhere and will enhance understanding of ecological response to changing conditions in Great Lakes estuaries.

The St. Louis River Estuary

The SLRE was formed when post-glacial isostatic rebound caused Lake Superior to rise in the northeast, flooding the lower portion of the St. Louis River at the southwestern end of the lake (Ojakangas and Matsch, 1982). The SLRE is a Great Lakes "rivermouth" ecosystem as defined by Larson et al. (2013). The 5000-ha estuary forms a section of the state border between Duluth, Minnesota and Superior, Wisconsin (Fig. 1). The estuary is at the terminus of the St. Louis River Basin (9250 km^2), but also receives discharge from several tributaries, the largest of which is the Nemadji River (1140 km^2 basin area). Land cover in the St. Louis River watershed is 94% forest, wetland, and water; 4% agriculture; and 2% developed.

Allouez Bay at the southeast end of the SLRE (Fig. 1) is a shallow, semi-enclosed embayment with minimal human development. Superior Bay is a lagoon formed behind a natural 16 km-long sand bar and is open to Lake Superior at its northwestern and southeastern end. The bay contains the outer Duluth–Superior Harbor, a large commercial seaport, with extensive ship channels and industrial development. St. Louis Bay includes the inner harbor and is likewise industrialized and channelized. It is shallower than Superior Bay and is less hydrologically influenced by Lake Superior. Spirit Lake, a large flooded backwater of the river, is generally shallow and undeveloped. Above Spirit Lake, the estuary is riverine.

Physical aspects of the SLRE relevant to this study are its relative shallowness (mostly <3 m deep outside of dredged shipping channels and slips), the general absence of coarse substrates except in the upper, riverine portion of the estuary (which is not included in this study), and the restricted open water period, usually from April through November. Estuary morphometry is irregular and fetch distances are highly variable. For the prevailing northeast wind, maximum fetch distance is ≈4.5 km. Tributaries to the Allouez Bay, the Nemadji River, and the Pokegama River (Fig. 1) drain highly-erodible clays deposited in Glacial Lake Duluth (Magner and Brooks, 2008) and these areas are generally more turbid than the rest of the SLRE (DeVore, 1978).

SAV beds are widespread across shallow areas of the SLRE. A vegetation survey of the SLRE conducted in 2010 (John Lindgren, MN DNR, unpublished data) collected 21 species of SAV at 688 sites. At sites where SAV was present, the most frequently collected species (present at 83% of sites) was American wild celery, *Vallisneria americana* Michx.

In June 2012, a 500-year recurrence interval flood occurred across the lower St. Louis River Basin (Supplementary Information Appendix A; Czuba et al., 2012). To evaluate the effects of this event on SAV, we resurveyed portions of Allouez Bay, St. Louis Bay, and Spirit Lake in 2012, post-flood. This aspect of our study was unplanned and opportunistic, but we include the results here because they provide insight into interannual variation in SAV across the SLRE.

Methods

Survey methods and instrumentation

Methods for sampling SAV include grab or rake sampling (Havens et al., 2002; Rodusky et al., 2005; Skubinna et al., 1995), direct observation by diving or video (Hudon et al., 2000), remote sensing (Narumalani et al., 1997; Wolter et al., 2005), photo interpretation (Zhu et al., 2007), and hydroacoustic methods (Depew et al., 2010). In the SLRE, SAV beds are often patchy, turbidity varies considerably among areas (DeVore, 1978) and over time, and the growing season is short. Given these conditions, hydroacoustic survey methods were the best option for generating the extensive, high resolution data needed for modeling.

From late July through mid September in 2011, we surveyed SAV in Allouez Bay, part of Superior Bay, eastern half of St. Louis Bay, and Spirit Lake (Fig. 1). Transects were aligned along gridlines plotted on a GPS unit (Garmin GPSMAP 536, Garmin International, Olathe, KS) aboard the survey vessel. Total survey transect length in 2011 was 365 km. In 2012, we resurveyed transects in each area during the same weeks as in 2011. The survey vessel was a 5.7-m long flat-bottomed aluminum boat with outboard power. Because of vessel size, the operational depth limit for the hydroacoustic survey was ≈0.5 m. This means that models based on our data should not be extrapolated to shallower depths.

Hydroacoustic instrumentation included narrow beam (6°), 120 and 420 kHz BioSonics transducers, and an onboard BioSonics DT-X digital echosounder (BioSonics Inc., Seattle, WA). Data were captured on a notebook computer using Visual Acquisition software (BioSonics, 2010). Hydroacoustic data for each GPS "fix" along each transect was summarized into SAV indicators for that GPS location. Many additional details of hydroacoustic methods and instrument and software settings used in this study are given in Supplementary Information Appendix B.

An underlying assumption of this method is that the digital signal is detecting SAV and is not systematically detecting something else. In areas of relatively shallow water, where SAV was visible from the boat, we could confirm that the transducer was passing over visible SAV beds or bare bottom from the display of digital signal from the echosounder. The reliability of this method for surveying aquatic vegetation has been demonstrated, and its use for this purpose is widespread (e.g., Depew et al., 2010; Sabol et al., 2009; Valley et al., 2005; Winfield et al., 2007).

Previous recent SAV sampling (Brady et al., 2010) and our own observations showed that SAV was almost never collected deeper than 2.5 m in the SLRE. We therefore excluded locations with a mean depth > 2.5 m to focus the predictive modeling on sources of variation in SAV in areas of the estuary within the depth range currently capable of supporting SAV.

Bottom typing parameters were extracted from digital data from the 120 kHz transducer using Visual Bottom Typer (VBT) V. 1.12 software (BioSonics, 2007). We retained three parameters related to substrate characteristics: E1, E1′, and fractal dimension (BioSonics, 2007). E1 is based on the first part of the bottom echo for a ping and may correspond to bottom roughness. E1′ is based on the second part of the bottom echo for a ping and may correspond to bottom hardness. Fractal dimension has been correlated with physical and chemical properties of bed sediment (Anderson and Pacheco, 2011).

We determined the fetch distance by wind direction for each location (0–360 in 10-degree increments) using the SPM-restricted method of Rohweder et al. (2008). Wave height is a function of fetch, wind speed, and wind duration (Keddy, 1982). The relative exposure index (after Keddy, 1982) integrates these variables into an index computed as the sum across wind directions of mean monthly wind for April–October from each direction multiplied by the proportion of the month that the wind was blowing from that direction, scaled from 0 to 1, and multiplied by the fetch distance for the direction. Hourly wind data were from Sky Harbor Airport on Superior Bay (46.7219 N, 92.0433 W). Bed slope in percent was calculated from bathymetry raster data (10 × 10 meter cell size) using the Slope tool in ArcGIS for Desktop 10.1 which is based on the average maximum technique (Burrough and McDonell, 1998).

We used the measured SAV percent cover at the location immediately previous to each useable record location along each transect as a lag variable to correct for possible serial autocorrelation of model error. SAV percent cover, substrate parameters, corrected depth, and exposure and bed slope data were combined in Arc-GIS.

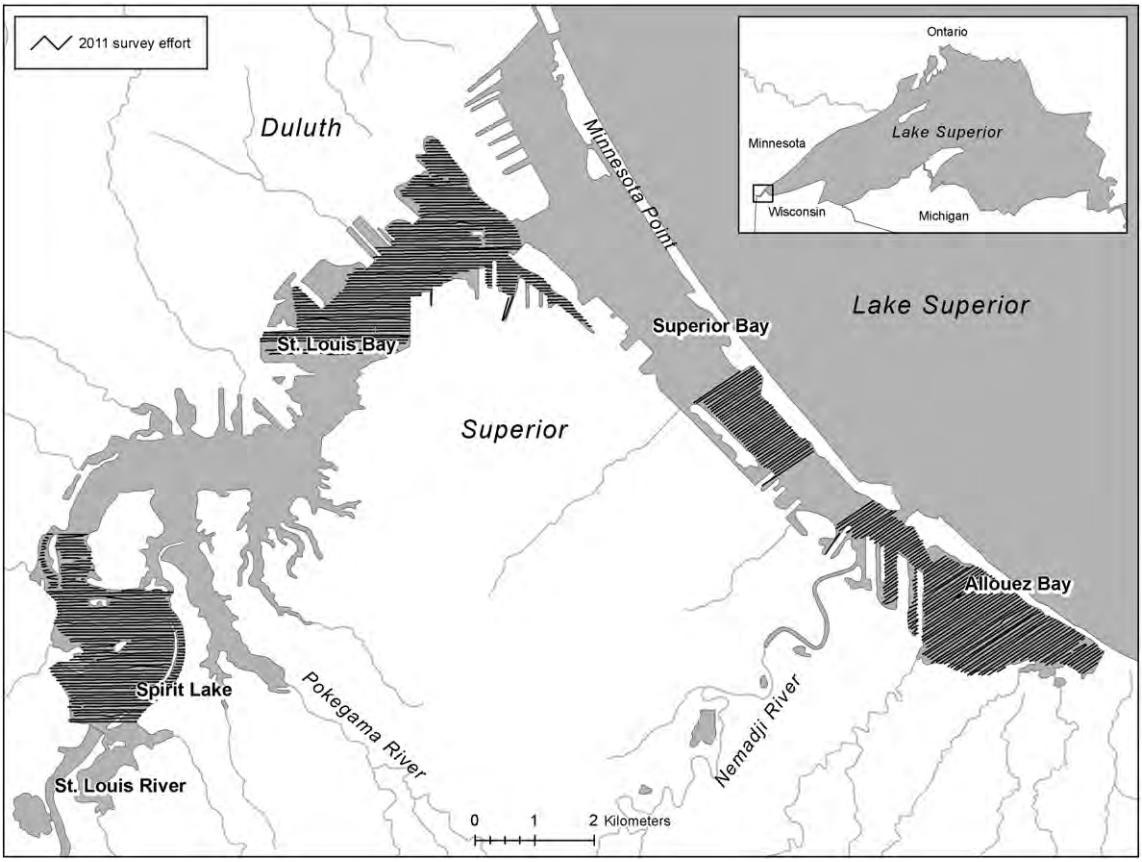

Fig. 1. Four areas of St. Louis River Estuary were surveyed in 2011: Allouez Bay, Superior Bay, St. Louis Bay, and Spirit Lake. Survey transects were aligned along a grid of GPS waypoints spaced 50 m apart. In Superior and Allouez Bay, transects were oriented northeast by southwest to run perpendicular to depth contours in this area. Elsewhere in the estuary, transects were oriented east by west.

Water quality and SAV grab sampling

At the start, midpoint, and end of approximately every fifth transect we collected a surface water grab sample for turbidity analysis. For a concurrent study, we collected water grab samples at random locations across the SLRE for determination of nutrient concentration. Water temperature was recorded every 15 min at 7 locations in the SLRE on HOBOTemp recording sensors. (Onset Computer Corporation, Bourne, MA). Turbidity was determined for each sample using an AquaFlour turbidimeter (Turner Designs, Sunnyvale, CA). Total nitrogen and total phosphorus concentrations were determined using a Lachat flow-injection analyzer (Hach Company, Loveland, CO). Unfiltered sub-samples were digested using the persulfate method (APHA, 1998). Turbidity, nutrient concentration, and temperature data were not included as predictors in SAV models, because they do not vary (and were not measured) at the same spatial scale as our hydroacoustic SAV data. Instead, we used this information to inform spatial stratification of the SLRE for data analysis and for interpreting the results.

At 124 locations within visible SAV beds distributed across the surveyed areas, we collected SAV samples (0.27 m^2) using tongs (after Rodusky et al., 2005). Samples were sorted to species, dried (105 °C), and weighed.

Substrate analysis

We examined echograms from selected locations in the SLRE to locate ≈150-ping segments of transects with visually uniform bottom type. We extracted the mean value of bottom type parameters (E1, E1′, and fractal dimension) for each segment using Visual Bottom Typer software. To calibrate the typing parameters we collected two standard PONAR samples (0.046 m^2) at each transect segment location (N = 50 locations). Each PONAR sample was subsampled, sieved, and dried (105 °C) to determine the percent of dry mass in the clay (<63 μm), fine (63–500 μm), sand (500 μm–2 mm), and coarse (>2 mm) fractions. Subsamples of each fraction were ashed (500 °C) to determine the percent of organic matter. We used rank correlation to determine if gravimetric substrate measurements in the calibration dataset were related to bottom typing parameters.

Cover models

Preliminary analysis revealed complex non-linear responses of percent SAV cover to predictors. We therefore used regression tree modeling (RTM, TREE program in SYSTAT v. 11) to examine sources of variation in SAV cover in each area of the SLRE. RTM is a non-parametric approach (Breiman et al., 1984) well suited to characterizing non-linear responses. Candidate predictors included depth, bed slope, relative exposure index, fractal dimension, E1, E1′, and lag percent cover. We randomly split the data in half into training and validation (holdout) datasets. We also excluded data from an area in Superior Bay to be used as an independent dataset for model validation. Using RTM, we split sample locations into groups that minimized within-group heterogeneity using a least squares loss function until the added proportional reduction in error (PRE) was <1%. The final groups are the terminal nodes of the regression tree. The cumulative PRE is equivalent to model r^2 (Wilkinson, 1998). We also created reduced regression tree models excluding lag cover and fractal

Table 1
Relative biomass and frequency (%) of submerged aquatic vegetation (SAV) species in grab samples collected at four sites within the SLRE in 2011. Mean total dry mass for each site is given at bottom of the table (g/m^2).

Taxon	Spirit Lake N = 44		St. Louis Bay N = 25		Allouez Bay N = 22		Superior Bay N = 33	
	Dry mass (%)	Samples (%)	Dry mass (%)	Samples (%)	Dry mass (%)	Samples (%)	Dry mass (%)	Samples (%)
Vallisneria americana Michx.	90	95	100	100	54	68	94	94
Potamogeton richardsonii (Benn.) Rydb.	3	14	0	0	46	59	0	0
Ceratophyllum demersum L.	1	5	0	0	0	5	0	0
Potamogeton sp.	0	0	0	0	0	5	3	3
Najas flexilis Willd.	4	7	0	0	0	0	3	9
Myriophyllum sp.	2	5	0	0	0	0	0	0
Mean total dry mass (g/m^2)	73		20		47		20	

dimension that could be applied to other locations in the SLRE using readily available bathymetry, morphometry, and wind data. We validated trees by dropping training, cross-calibration, and independent (Superior Bay) data through the regression tree and examining the rank order of the terminal means.

Occurrence models

We created logistic regression models for each area of the SLRE to predict the probability of SAV being present at each report location. We created models for the training dataset using the Logistic procedure in SAS v. 9.1 with stepwise elimination ($\alpha = 0.05$). Plots of cover by depth for selected predictor values (Supplementary Information Appendix C) suggested that interactions between depth and other predictors were likely to be significant, and so were included in regression models. We retained the main effect if their interaction terms were significant in the model. We examined the performance of the models using the area under the receiver operating characteristic (AUROC) curve. AUROC is the probability of concordance between random pairs of observations and ranges from 0.5 to 1 (Gönen, 2006). We cross-validated logistic occurrence models for their ability to classify correctly locations in the validation (holdout) dataset and in the Superior Bay dataset. For classification, we converted log odds from the model to probability of SAV occurrence using the logistic function. We then converted model-predicted probability of SAV occurrence ($\hat{y}_{SAV}$) to binary predictions (i.e., $\hat{y}_{SAV} > 0.5 = 1$, $\hat{y}_{SAV} \leq 0.5 = 0$). Assessed accuracy was the percent of all records where the predicted value and actual value agreed either as true positive (1, 1) or true negative (0, 0). Percent false positives (prediction = 1, actual = 0) or false negatives (prediction = 0, actual = 1) were also determined. We created reduced occurrence models to allow us to simulate predictor effects when the gear-specific substrate predictor (fractal dimension) and the autocorrelation variable (lag SAV) were excluded. We cross-validated reduced models as described above. We further validated reduced models using an independent dataset collected by the Natural Resources Research Institute (NRRI; Brady et al., 2010; Host et al., 2012) using rake sampling methods (MN DNR, 2012). We extrapolated bed slope and relative exposure index for NRRI sample locations using the methods described above. We also created regression tree models (TREE program in SYSTAT v. 11) as described above for SAV cover except with SAV occurrence (1 or 0) as the response variable.

Results

SAV species composition

American wild celery (*V. americana*) was the most common species collected by dry weight and frequency of occurrence in our samples (Table 1). Wild celery was the only SAV species we collected in St. Louis Bay. Clasping-leaved pondweed, *Potamogeton richardsonii* (Benn.) Rydb., was co-dominant with wild celery in Allouez Bay. Across the SLRE, SAV species diversity was higher in sheltered areas than in more exposed areas.

Water quality variation among areas

Mean turbidity in Allouez Bay, 67 NTU, was much higher than other areas of the SLRE (<10 NTU) in 2011 (Fig. 2). Mean turbidity generally decreased slightly up-estuary and was lowest in Spirit Lake. Total N and total P concentration, and mean temperature were slightly higher in St. Louis Bay and Spirit Lake than in Superior Bay or Allouez Bay.

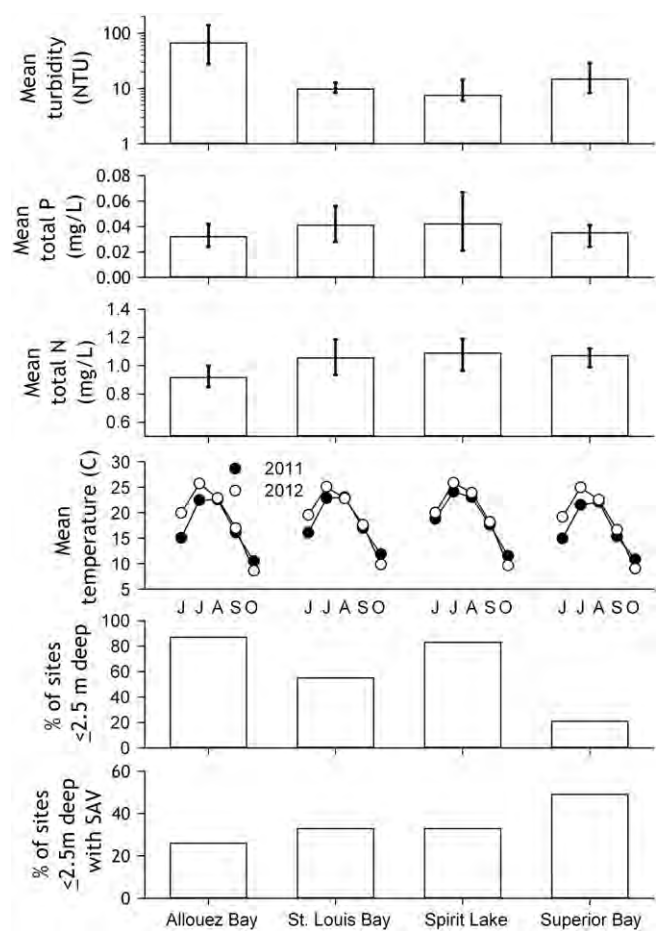

Fig. 2. Variation in turbidity, nutrient concentration, temperature, depth, and SAV occurrence among survey areas in the SLRE in 2011 (and 2012 for temperature). Values for nutrients are means ± range (N = 5, 14, 12, 3 for Allouez Bay, St. Louis Bay, Spirit Lake, Superior Bay respectively). Values for temperature are monthly means (June–October 2011). Values for turbidity are means ± range (N = 74, 89, 59, 73 for Allouez Bay, St. Louis Bay, Spirit Lake, Superior Bay respectively).

SAV cover and occurrence

About 60% of the surveyed locations of the SLRE were shallow (<2.5 m, Fig. 2). Superior and St. Louis Bays were the deepest areas with ≤55% of the surveyed area shallower than 2.5 m (Fig. 2). Spirit Lake and Allouez Bay were the shallowest areas with ≥83% of the surveyed area shallower than 2.5 m.

The percent occurrence of SAV in water shallower than 2.5 m was highest in Superior Bay (49%) and lowest in Allouez Bay (26%). Where it occurred, SAV cover was not continuous at the scale we measured. Mean percent cover (i.e., within SAV beds) ranged from 31% in Spirit Lake to 41% in Allouez and Superior Bays (Fig. 3).

SAV predictors

Across locations <2.5 m deep (the threshold depth for modeling), mean depth, relative exposure index, bed slope, and fractal dimension varied between locations with and without SAV (Fig. 3). Except for relative exposure index in Allouez Bay, the difference between locations with and without SAV was significant (t-test $p < 0.05$). For all areas, locations with SAV were shallower and had finer substrate (higher fractal dimension) than locations where SAV was absent (Fig. 3). The patterns for relative exposure index and bed slope were not consistent among areas.

The bottom typing parameters E1 (first part of bottom echo) and E1′ (second part of bottom echo) were strongly correlated with depth ($r_s \geq 0.92$, Supplementary Information Appendix D.1). Fractal dimension was less strongly correlated with depth, positively correlated with percent clay and negatively correlated with other particle size fractions. Correlations among predictors from the survey confirm the strong relationship of E1 and E1′ with depth ($r_s = 0.68$–0.90, Supplementary Information Appendix D.2). We therefore excluded E1 and E1′ from the models. Correlations among predictors were otherwise weak ($|r_s| \leq 0.3$, Appendix D.2).

Relationships between percent cover and predictors were non-linear (Fig. 4). Percent SAV cover did not vary much with change in depth deeper than 2.25 m. Mean percent cover declined at depths shallower than ≈1.2 m in St. Louis Bay and Spirit Lake. Cover did not vary with change in fractal dimension below 1.0. Range in mean cover across the range of bed slope (≈0–30%) was small, <10%. The relationship between mean relative exposure index and cover was variable. In St. Louis Bay, however, mean SAV cover declined with relative exposure index above and below 7500.

SAV cover models

Cumulative proportional reduction in error (PRE; $\approx r^2$) in regression tree models ranged from 0.29 to 0.53 (Table 2). Most of the reduction in error was from branching into lag cover groups followed by depth. The best reduced regression tree model (fractal dimension and lag cover excluded) was for St. Louis Bay (PRE = 0.36, Table 2, Supplementary Information Appendix E.1). The St. Louis Bay reduced regression tree model divided locations into depth groups of <1.5 m with a mean SAV cover of 28% and ≥1.5 m with a mean SAV cover of 3% (PRE = 0.28). The shallow group was split into a high relative exposure index group (>3133) with a mean cover of 33% and a low exposure group (<3133) with a mean cover of 21% (PRE = 0.02). The rank of node means for the St Louis Bay validation data matched the node means for the data on which the mode was based (Supplementary Information Appendix E.1). Because the areas differed significantly in morphometry (see relative exposure index in Fig. 3), high relative exposure index nodes 4 and 6 were empty for the Superior Bay validation data. Ranks were otherwise similar to the model training data indicating that the St. Louis Bay model was reliable for independent data.

SAV occurrence models

SAV occurrence was significantly related to linear combinations of predictor variables (all models $p < 0.001$; $r^2 = 0.30$–0.62, Table 3) for all areas. Lag presence/absence was the most important predictor (based on the Wald X^2 statistic). Logistic occurrence models for St. Louis Bay and Spirit Lake were similar to each other relative to the Allouez Bay model. For example, the signs of model coefficients of depth, relative exposure index, depth x relative exposure index

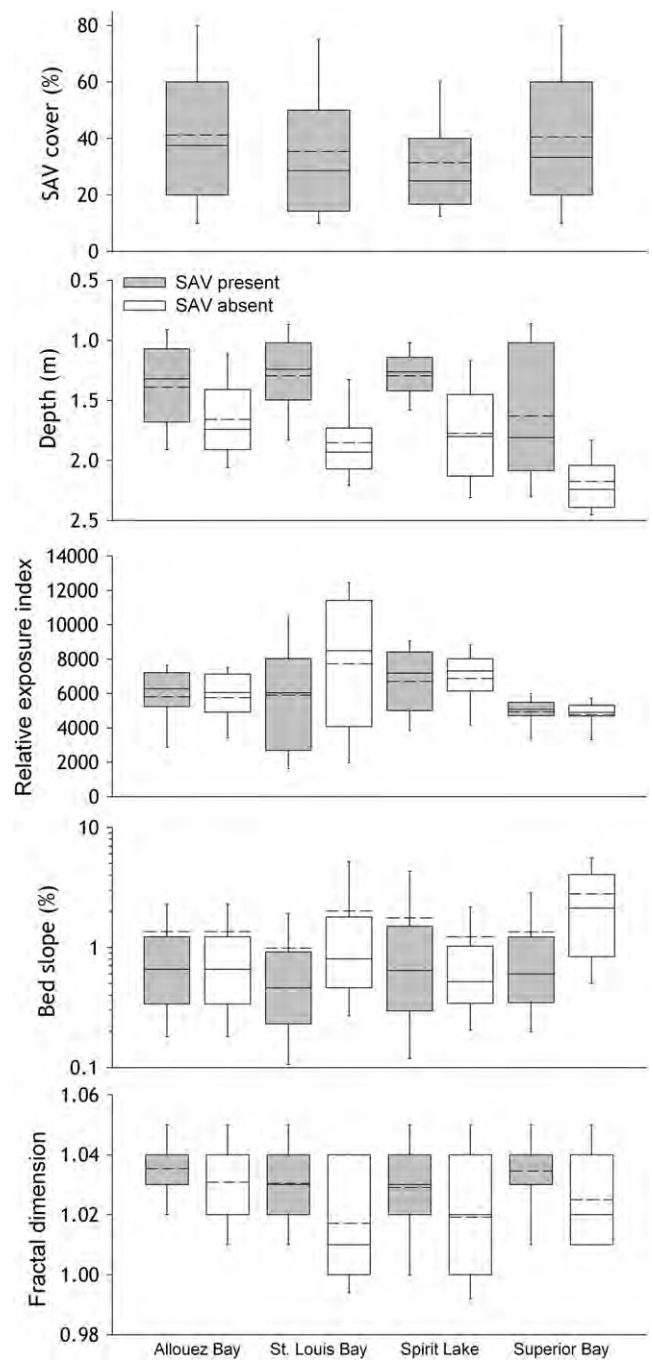

Fig. 3. Variation in predictors and percent cover among areas and between locations within areas with and without SAV in the SLRE in 2011. Box plots show 10th and 90th percentiles (whiskers), 25th and 75th percentiles (boxes), medians (solid horizontal line), and means (dashed line). N (number of locations) for SAV present/SAV absent = Allouez Bay 4954/13,952; St. Louis Bay 5446/11,526; Spirit Lake 5523/8516; Superior Bay 945/965).

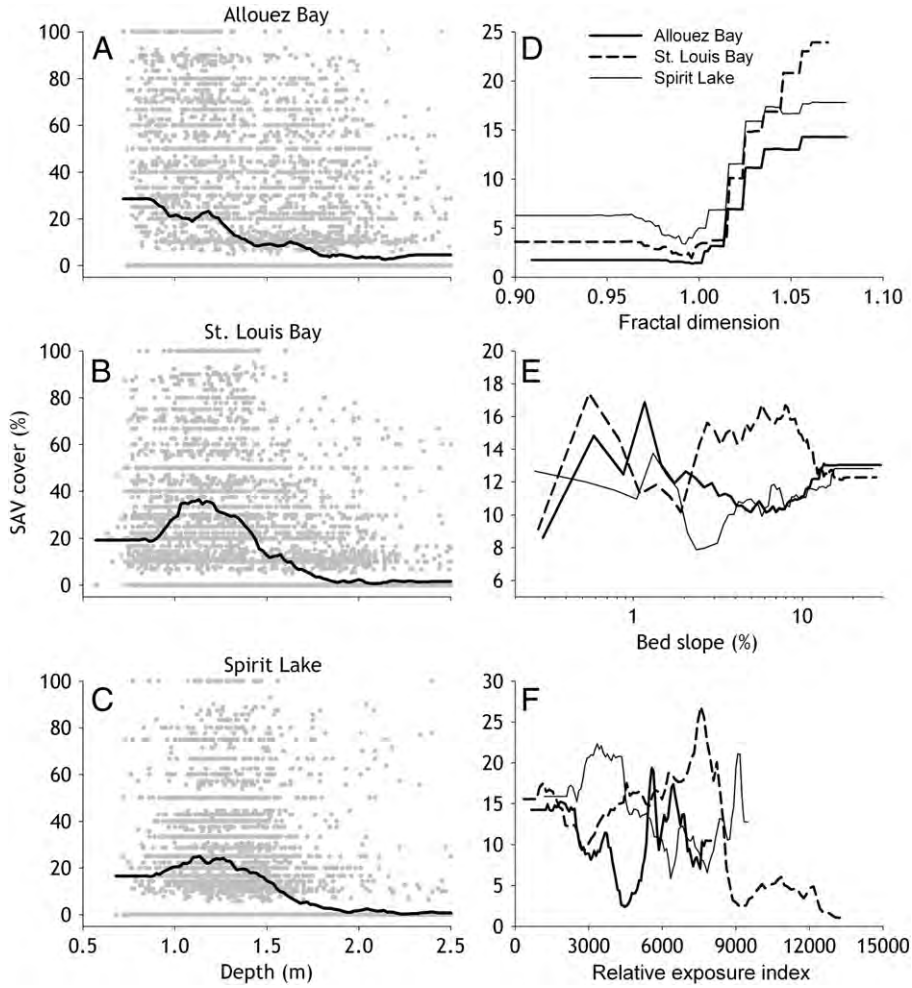

Fig. 4. Panels A–C: Scatter plots of percent SAV cover in study areas in SLRE in 2011 by depth for Allouez Bay (A), St. Louis Bay (B) and Spirit Lake (C). Lines are running averages (sample proportion = 0.05). Panels D–F: running average plots (sample proportion = 0.05; scatter plots not shown) for fractal dimension (D), bed slope (E), and relative exposure index (F).

interaction, and depth x fractal dimension interaction were different for Allouez Bay and the two other areas.

Model performance, as indicated by the area under the receiver operating characteristic (AUROC) curve was >0.8 (Table 3). Assessed accuracy of models (the percent of records where the predicted probability of occurrence and actual SAV presence or absence agreed) for split datasets was 79% for Allouez Bay, 86% for St. Louis Bay, and 78% for Spirit Lake (Supplementary Information Appendix E.2). Assessed accuracy of the St. Louis Bay model for Superior Bay was 74%. In St. Louis Bay and Spirit Lake the percent misclassification by false positive (predicting SAV occurrence when it is absent) and false negative was ≤56%. In Allouez Bay, more misclassifications were due to false negatives (72%). For the St. Louis Bay model (the most accurate of the fully parameterized models), the effect of relative exposure on probability was significant as was the interaction of depth and exposure. The positive effect of exposure on SAV occurrence decreased with increasing depth.

Reduced occurrence models without lag cover or fractal dimension (Table 4) were slightly less accurate than the full models (75–82%). As for the full models, the model for St. Louis Bay was the most accurate (82%). Assessed accuracy of the St. Louis Bay reduced model for classifying Superior Bay locations was 68%. In Allouez Bay, the negative effect of relative exposure on SAV occurrence increased with depth. In St. Louis Bay, the positive effect of relative exposure decreased with depth. In Spirit Lake, the bed slope had a negative effect on probability of SAV occurrence, and the effect increased with depth.

Mean depth, relative exposure index, and bed slope for the "population" of locations sampled by us in 2011 (on which our models were based), and the rake sample sites sampled in 2010 and 2011 by NRRI (Brady et al., 2010; Host et al. 2012) were somewhat different (Table 5). The sites rake sampled in St Louis Bay were, on average, significantly shallower and less exposed (lower relative exposure index) than locations we surveyed. In Spirit Lake, bed slope at rake sample sites was less than where we surveyed. Despite these differences, our models were 68% accurate at classifying rake sample sites as SAV is present or absent for St. Louis Bay, and 85% accurate for Spirit Lake (Table 5). Most misclassifications (73–100%) were false negatives wherein our models failed to predict SAV at sites where rake samples indicated SAV was present.

Lag cover and depth accounted for most reduction in error in regression tree models (Table 2). As for cover models, the best occurrence models were for St. Louis Bay. The St. Louis Bay reduced model (Appendix E.2) divided locations into shallow locations (<1.5 m) with a mean SAV probability of occurrence of 0.71 and deeper locations (>1.5 m) with a mean SAV probability of occurrence of 0.12 (PRE = 0.36). The deep group was further split into shallow group (<1.74 m) with a mean SAV probability of 0.34 and a deeper group (≥1.74 m) with a

mean probability of occurrence of 0.07 (PRE = 0.03). The St. Louis Bay SAV occurrence regression tree accurately classified cross validation data (Supplementary Information Appendix E.2). The model performed reasonably well for Superior Bay data, but over-predicted the probability of occurrence in node 3 (locations 1.5–1.74 m deep with relative exposure index >5138) relative to the training data.

June 2012 flood

On June 21, 2012, following a 2-day, 18-cm precipitation event (Czuba et al., 2012), maximum daily discharge from Fond du Lac Dam at the head of the SLRE was over 1600 m^3/s. Normal June baseflow is ≈100 m^3/s (Supplementary Information Appendix A). This event followed a smaller storm in May during which flows in the St. Louis River were also elevated. Reliable turbidity data are not available for this period, but we observed elevated turbidity across the SLRE from late May through July 2012. For the three areas we resurveyed in 2012 after the flood, percent SAV cover and occurrence were lower than in 2011 (Fig. 5). Percent cover declined by >60% in St. Louis Bay and Spirit Lake and 31% in Allouez Bay. Percent of location <2.5 m deep with SAV declined by >75% in St. Louis Bay and Spirit Lake and 41% in Allouez Bay.

We examined the accuracy of the reduced occurrence models (Table 4) in predicting SAV occurrence after the flood. Model accuracy in Spirit Lake was very poor after the flood, correctly classifying only 44% of locations (Table 4). The majority of classification errors (88% in St. Louis Bay and 96% in Spirit Lake, Table 4) were false positives—the model predicted SAV would be present and it was not.

Discussion

SAV and depth

Based on the mean percent submerged aquatic vegetation (SAV) cover, maximum rooting depth of SAV in the St. Louis River Estuary (SLRE) in 2011 was ≈2.1 m. Optimal depth, below which the probability of SAV occurrence declines rapidly, was ≈1.2 m in St. Louis Bay and Spirit Lake and <1 m in more turbid Allouez Bay. This depth range for St. Louis Bay and Spirit Lake is similar to published values for wild celery from waters with similar turbidity. For example, on the Upper Mississippi River (15 NTU) wild celery was most abundant at 0.5–1.1 m (Kreiling et al., 2007). On the Detroit River (5–10 NTU), the species was most abundant at 0.3–1.5 m (Hunt, 1963). Wild celery can grow deeper (>2.5 m) in more transparent waters (Catling et al., 1994), and presumably would do so in the SLRE where turbidity was lower.

We could not determine minimum SAV depth in the SLRE because of our sampling method. However, we observed that in water shallower than 0.5 m, SAV gives way to bare sand in the exposed areas. We do not know if this is due to the limitation of plants by direct wave action or to the effect of wave erosion on sediment characteristics (Duarte and Kalff, 1990). In more sheltered areas, SAV beds transition to a mixture of SAV, floating, and emergent vegetation as water shoals. Wilson and Keddy (1986) postulated diversity–disturbance relationship for shoreline plant assemblages wherein disturbance limits competitive dominance. This may account for our observation that in more sheltered areas, caulescent SAV, floating-leaved, and emergent species occupy depths at which wild celery would likely dominate elsewhere in the SLRE in more exposed locations.

Predictive models

The physical habitat and water quality data confirm the appropriateness of the area-specific modeling approach for the SLRE. Allouez Bay was much more turbid than the other areas and had a different SAV assemblage. Turbidity was similar in St. Louis Bay and Spirit Lake, but the water depth and exposure were higher in St. Louis Bay than Spirit Lake.

Lag cover and depth accounted for the most variation in SAV cover in all areas. When lag cover was excluded, exposure (i.e., relative exposure index) became significant. The best regression tree cover models were for St. Louis Bay where percent cover was highest (36%) in water shallower than 1.5 m and where relative exposure index was >11,490. This positive effect of exposure is discussed below.

The SAV cover and occurrence models were least accurate for Allouez Bay, possibly due in part to the nature of the SAV assemblage there. Wild celery in Allouez Bay is mostly restricted to a narrow band between emergent vegetation (to landward) and open water or patches of clasping-leaved pondweed. We surmise that pondweed, a caulescent "canopy-forming" species that concentrates photoreceptive biomass near the water surface (Barko et al., 1984; Best et al., 2008), can outcompete wild celery, a "meadow-forming" species, for light in much of Allouez Bay since it is less constrained to a narrow depth range. In Allouez Bay, clasping-leaved pondweed does not seem to grow in beds like wild celery, but in more widely distributed patches and therefore may not be as easily modeled at the fine spatial scale of our data.

Based on independent rake sampling of the SLRE (Brady et al., 2010; Host et al., 2012) the ability of our reduced models to classify correctly locations as SAV present or absent was 85% for Spirit Lake and 67% for St. Louis Bay (Table 5). In St. Louis Bay, our models were based on transects through locations that were, on average, more exposed (higher relative exposure index) and deeper than the rake sample locations. Our models probably underestimate the extent of SAV sheltered areas of the SLRE, possibly because, due to inaccessibility, these areas were underrepresented in the original survey on which the models were based. Also, in shallow sheltered areas, floating-leaved and emergent vegetation, which increase the amount of noise in the SAV data (Supplementary Information Appendix B), tend to co-occur with SAV.

The inclusion of a lag variable improved the performance of the occurrence models, as would be expected. Our interpretation is that many SAV patches (and gaps between patches) were large enough to overlap the bottom area covered by successive reports (which were 3.9 m apart; see Supplementary Information Appendix B). Wild celery is capable of sexual and asexual reproduction. Clonal growth (Catling et al., 1994) and a short seed-dispersal distance (Kaul, 1978) may constitute contagious biological processes (sensu Legendre, 1993) within wild celery beds that account for the non-independence of locations along each transect.

Table 2
Regression tree model results for SAV in the SLRE in 2011 showing proportional reduction in error (PRE) in response variable for predictor at three sites.

SAV response variable	Predictor	Allouez Bay	St. Louis Bay	Spirit Lake
		Proportional reduction in error (PRE)		
Cover	Lag cover	0.26	0.47	0.31
	Depth	0.03	0.05	0.06
	Fractal dimension	0.00	0.00	0.01
	Cumulative PRE (r^2)	0.29	0.53	0.38
	Reduced models			
	Depth	0.11	0.31	0.22
	Relative exposure index	0.06	0.05	0.00
	Cumulative PRE (r^2)	0.17	0.36	0.22
Occurrence	Lag cover	0.17	0.42	0.06
	Depth	0.03	0.08	0.34
	Fractal dimension	0.00	0.01	0.00
	Cumulative PRE (r^2)	0.20	0.51	0.40
	Reduced models			
	Depth	0.10	0.39	0.34
	Relative exposure index	0.04	0.03	0.00
	Cumulative PRE (r^2)	0.14	0.42	0.34

Table 3
Stepwise logistic regression occurrence model results. Dependent variable is log probability of SAV occurrence. Model $p < 0.001$ in all cases. Classification accuracy (SAV probability >0.5 when SAV is present (P) and SAV probability ≤0.5 when SAV is absent (A)) is based on cross-validation using a split dataset. Lag SAV P/A is the presence (1) or absence (0) of SAV at the previous location on the transect. AUROC is the area under the receiver-operating characteristic curve; AUROC ranges from 0.5 (random prediction) to 1 (perfect classification). REI = relative exposure index. Accuracy percentages in parentheses are for independent Superior Bay data.

Model parameters	Allouez Bay (N = 9323)		St. Louis Bay (N = 8212)		Spirit Lake (N = 6211)	
	Estimate	Wald X^2	Estimate	Wald X^2	Estimate	Wald X^2
Intercept	−44.19		−6.11		−1.37	
Depth	18.15	10	−16.29	14	−11.78	4
REI	−0.0004	43	0.0005	121	0.0003	13
Bed slope	−0.21	27	−0.03	ns	−0.32	22
Fractal dimension	45.99	31	6.47	ns	3.93	ns
Lag SAV P/A	1.57	784	1.85	621	1.20	279
Depth x REI	0.0004	66	−0.0003	113	−0.0002	10
Depth x bed slope	0.20	59	0.06	6	0.22	28
Depth x fractal dimension	−21.33	15	14.58	12	9.03	3
Model performance and validation						
Likelihood ratio	2116		4759		3023	
Nagelkerke r^2	0.30		0.62		0.52	
AUROC (0.5–1)	0.80		0.92		0.88	
Accuracy (%)	79		86 (74)		78	
True positive (%)	13		28 (35)		35	
True negative (%)	87		72 (65)		65	
False positive (%)	28		44 (10)		53	
False negative (%)	72		56 (90)		47	

In St. Louis Bay and Spirit Lake, the positive effect of relative exposure index on probability of SAV occurrence increased with decreasing depth (see Supplementary Information Appendix C). We think that the dominant SAV, a wild celery, a deep-rooted species (Wigand et al., 2000), is adapted to persist within the normal limits of the fetch-disturbance regime of the SLRE. This interaction probably owes to the competitive advantage wild celery has over emergent and floating-leaved species when relative exposure index is high. In Lakes Mendota and Wingra, Wisconsin, Titus and Adams (1979) found that the rooting system of wild celery allowed it to resist replacement by Eurasian water-milfoil, *Myriophyllum spicatum* L. in shallow water subject to wave action. Stewart et al. (1997) found that canopy-forming SAV species (e.g., Eurasian water-milfoil, and clasping-leaved pondweed) were more susceptible to wave damage than wild celery with its basal rosette growth-form. Kreiling et al. (2007) observed that wild celery biomass on the Upper Mississippi increased with increasing wind fetch, which they attributed to lack of competition from macrophyte species, which were intolerant of turbulence. Spence (1982) noted that SAV species diversity was usually higher in sheltered areas than in exposed areas.

Duarte and Kalff (1986) predicted maximum submerged macrophyte biomass in Lake Memphremagog (Vermont–Quebec) using a linear model including littoral slope which was negatively related and sediment organic matter which was positively related to SAV biomass. They felt that reduced sediment stability on steep slopes rather than an effect of slope on wave action accounted for the slope effect. In the SLRE, there was a significant interaction between slope and depth in Spirit Lake and Allouez Bay, and the negative effect of slope on SAV increased with depth. The mechanism underlying the slope effect in the SLRE is not clear.

Substrate fractal dimension was a significant predictor in our full models. In St. Louis Bay and Spirit Lake, the positive effect of fractal dimension on SAV occurrence increased with depth. The fractal dimension is a digital characterization of the acoustic bottom signal that is associated with substrate characteristics rather than a measure of them. Our analysis (Supplementary Information Appendix D) corroborates Anderson and Pacheco (2011). Like us, they found fractal dimension to be positively correlated with percent clay and negatively correlated with percent sand in bed sediments.

American wild celery, the dominant species in most of the SLRE, can apparently thrive in a variety of substrates from hard clay to gravel (Catling et al., 1994; Korschgen and Green, 1988). Hunt (1963) reported that the species grew best in silty sand in the Detroit River. Louvet-Doust and LaPorte (1991) reported a high wild celery density in clay sediment. On the Upper Mississippi River, wild celery grew on a variety of substrates (Korschgen and Green, 1988). Given this apparent indifference of the dominant SAV species to substrate type, it is difficult to interpret the meaning of the relationships between fractal dimension and SAV in the SLRE, beyond the fact that fractal dimension was associated with some aspect of the substrate that is related to the suitability for SAV. An implication for SLRE habitat restoration is that emplaced substrates should at least, to the degree possible, reflect the particle distribution of native sediments where SAV already occurs.

We did not measure nutrient concentration at the same scale as SAV cover, but we doubt that variation in nutrient concentration across the SLRE, which was relatively slight (Fig. 2), contributed much to variation in SAV distribution. There are many examples of large-scale SAV models that are driven primarily by nutrient concentration or loads (e.g., Cerco and Moore, 2001; Orth et al., 2010). Water quality varies significantly among Great Lakes coastal ecosystems (Croft and Chow-Fraser, 2007; Trebitz et al., 2007). Therefore, models of spatial variation in SAV among Great Lakes coastal ecosystems, or of temporal variation in SAV through time, will likely include water quality predictors such as nutrient concentration and turbidity.

We have ignored some factors for which we lack empirical data that might influence the distribution of SAV in the SLRE. For the predictive models described herein, these unmeasured sources of variation, including herbivory by waterfowl, ice scour, and phytotoxicity of contaminants contribute to model error. Our observations in the SLRE convince us that the effects of waterfowl foraging and ice scour on SAV are at most localized. Reschke and Host (2013) have recently presented preliminary evidence that sediment or water column contamination may be influencing the distribution of aquatic vegetation in the SLRE.

Table 4
Stepwise logistic regression results for reduced models (lag and fractal dimension omitted). Model $p < 0.001$ in all cases. Dependent variable is log probability of SAV occurrence. Accuracy (percent of cases where SAV probability >0.5 when SAV was present (P) and SAV probability ≤0.5 when SAV was absent (A)) is based on cross-validation using a split dataset. AUROC is the area under the receiver-operating characteristic curve; AUROC ranges from 0.5 (random prediction) to a 1 (perfect classification). Accuracy percentages in parentheses are for independent Superior Bay data; percentages in brackets are for transects resurveyed in 2012. REI = relative exposure index.

Model parameters	Allouez Bay (N = 9422)		St. Louis Bay (N = 8484)		Spirit Lake (N = 7020)	
	Estimate	Wald X^2	Estimate	Wald X^2	Estimate	Wald X^2
Intercept	5.55	218	0.99	22	5.92	1306
Depth	−5.17	335	−1.06	55	−4.23	1427
REI	−0.0005	86	0.0008	366		
Bed slope	−0.26	51			−0.46	103
Depth x REI	0.0005	125	−0.0005	356		
Depth x bed slope	0.23	110			0.29	115
Model performance and validation						
Likelihood ratio	1206		3646		2616	
Nagelkerke r^2	0.18		0.48		0.42	
AUROC (0.5–1)	0.73		0.87		0.83	
Accuracy (%)	75 [66]		82 (68) [79]		76 [44]	
True positive (%)	6 [8]		25 (26) [19]		35 [27]	
True negative (%)	94 [92]		75 (74) [81]		65 [73]	
False positive (%)	15 [31]		39 (4) [88]		49 [96]	
False negative (%)	85 [69]		61 (96) [12]		51 [4]	

Table 5
Comparison of predictor values and validation results for the reduced SAV occurrence model applied to an independent dataset. Classification accuracy (SAV probability >0.5 when SAV present (P) and SAV probability ≤0.5 when SAV was absent (A)) is based on model validation using an independent dataset collected in the SLRE in 2010 and 2011 by the Natural Resources Research Institute (NRRI, Brady et al., 2010; Host et al., 2012). Comparison in predictor means between this study and NRRI data was based on two sample *t*-tests with unequal variances. REI = relative exposure index; nsd = not significantly different.

Predictor	St. Louis Bay					Spirit Lake				
	This study N = 8486		NRRI N = 192		*t*-test	This study N = 7020		NRRI N = 65		*t*-test
	Mean	95% CI	Mean	95% CI	*p*	Mean	95% CI	Mean	95% CI	*p*
Depth (m)	1.68	1.67–1.69	1.46	1.39–1.53	<0.001	1.58	1.57–1.59	1.53	1.39–1.66	nsd
REI	7158	7078–7238	6605	6103–7108	<0.05	6818	6774–6863	6705	6254–7156	nsd
Bed slope (%)	1.87	1.80–1.94	1.51	1.10–1.92	nsd	1.32	1.26–1.37	0.79	0.63–0.95	<0.001
Model validation										
Accuracy (%)					68					85
True positive (%)					51					58
True negative (%)					49					42
False positive (%)					27					0
False negative (%)					73					100

Difference in SAV between 2011 and 2012

We infer that the decline in SLRE SAV in 2012 relative to 2011 was due to conditions during the winter of 2011–2012 or during the spring 2012 flood that was unsuitable for germination and survival of over wintering wild celery buds or seeds. Among the possible mechanisms are insufficient light (Korschgen et al., 1997), burial by deposited sediment (Carter et al., 1985), scour (Spink and Rogers, 1996), or too-cold water temperatures (Catling et al., 1994).

SAV declined more between 2011 and 2012 in Spirit Lake and St. Louis Bay than in Allouez Bay. The upriver areas lie downriver from a relatively confined river reach (Fig. 1) where flood energy would have been higher than in Allouez Bay. We did not observe extensive sediment deposition after the flood, and spring water temperatures were warmer in 2012 than in 2011 (Fig. 2). We are therefore inclined toward flood scour and decreased light availability through the spring and early summer after the flood as the reason for the decline in SAV cover and occurrence in 2012. Floods may cause long-term changes in riverine aquatic plant communities (Bornett and Puijalon, 2011). Our short-term findings for Spirit Lake and St. Louis Bay may represent the maximum interannual variation in SAV cover and occurrence likely to occur in the SLRE.

Habitat restoration and future conditions

The SAV occurrence regression trees are more intuitive than the logistic model results and produce broadly similar predictions, but they contain much less detail. For example, the reduced regression tree model for St. Louis Bay predicts that the mean probability of occurrence will be 0.79 when depth is <1.5 m and relative exposure index is >3134. Simulations based on the logistic regressions allow prediction of SAV occurrence for a range of depths and relative exposure index in the SLRE.

Simulations for St. Louis Bay and Spirit Lake (Fig. 6), two areas within the SLRE for which future habitat restoration is anticipated (SLRCAC, 2002) show conditions favorable for SAV, defined as a predicted probability of SAV presence ≥0.5. In St. Louis Bay, the maximum favorable depth was 1.1–1.6 m depending on exposure. In Spirit Lake, maximum favorable depth was 1.3–1.4 depending on bed slope. In St. Louis Bay, probability of SAV occurrence in shallow water (e.g., <1 m) was much higher when relative exposure index was higher than when relative exposure index was low. We hypothesize that at shallow exposed locations, only wild celery can persist; at more sheltered locations SAV, floating, and emergent vegetation are intermixed.

Because our reduced SAV occurrence models do not include a specialized sediment predictor or require knowledge of existing SAV conditions (e.g., lag), they are more generally applicable for simulations related to restoration or protection of SAV beds in the SLRE. They will allow users, for example, to predict and map SAV occurrence at unsurveyed locations in the SLRE using only bathymetric, morphometric (fetch), and wind data, to predict vegetation responses to restoration, or to predict how future changes in water level and changes in fetch (e.g., due to creation, immersion, or emersion of islands) may affect the distribution of SAV in the SLRE.

Seventeenth and eighteenth century travelers in the SLRE described a wide shallow river with wetland vegetation so extensive as to obscure the path of the main river channel (SLRCAC, 2002). Since then, much of the estuary has been dredged for navigation to a depth of 8.2 m. Isostatic rebound has caused the Lake Superior Basin to tilt downward to the southeast, gradually deepening the estuary (SLRCAC, 2002). The net result has been an increase in open water at the expense of wetlands. We speculate that accompanying this change has been the increase in baseflow turbidity caused in part by the lost sediment trapping function of emergent wetlands and SAV and increased resuspension of deposited sediments in the now largely open water reaches of the lower estuary.

The effect of climate change on future river flow and Lake Superior water level is uncertain, although most projections are of a decrease in

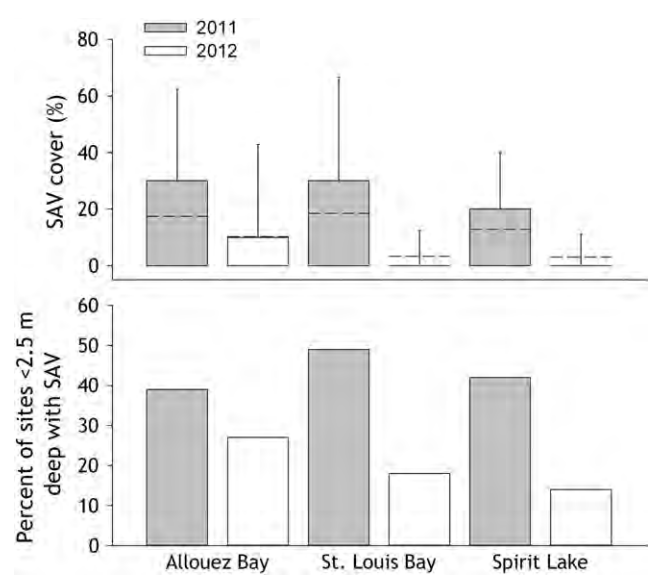

Fig. 5. Change in percent SAV cover and occurrence between 2011 and 2012 in the SLRE (following a large flood). Box plot shows 10th and 90th percentiles (whiskers), 25th and 75th percentiles (boxes), medians (solid horizontal line), and means (dashed line) (N for 2011/2012 = Allouez Bay 7993/7540; St. Louis Bay 3119/3734; Spirit Lake 5433/8153.

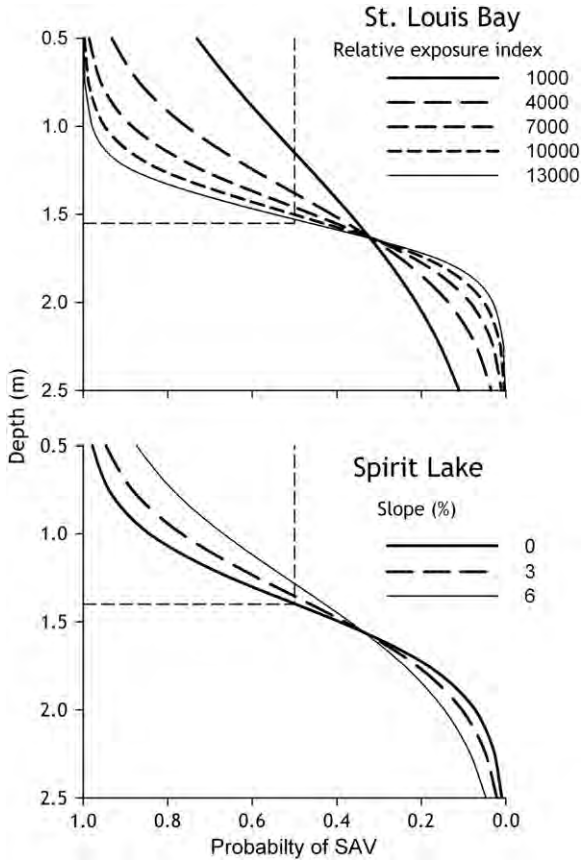

Fig. 6. Simulations based on reduced logistic regression models (lag SAV and fractal dimension excluded from models) for two areas of the SLRE. St. Louis Bay: the effect of depth on probability of SAV occurrence for a range of relative exposure index values. Spirit Lake: the effect of depth on probability of SAV occurrence for a range of bed slope values. Vertical dashed line indicates 50% SAV cover the threshold adopted for likely successful restoration; horizontal dashed line indicates values of depth and and relative exposure index at which 50% SAV cover would be realized.

lake levels (Angel and Kunkel, 2010; IUGLS, 2012). Planned and future restoration of shallow-water habitat in the SLRE should accommodate this future uncertainty by providing a range of depth and exposure combinations over native sediments so that SAV, floating, and emergent vegetation, once established, can adjust its distribution to future conditions.

Acknowledgments

Megan McGuire, Will Bartsch, and Pat Collins provided field support. Debra Taylor identified SAV plant specimens. Colleen Elonen and Lindsey Monson analyzed water samples. Christopher Patrick and Heidi Langrehr provided comments on the manuscript. Bob Stevens provided IT support. The views expressed in this article are the authors' and do not necessarily reflect EPA policy.

Appendix A. Supplementary data

Supplementary data to this article can be found online at http://dx.doi.org/10.1016/j.jglr.2013.09.013.

References

Anderson, M.A., Pacheco, P., 2011. Characterization of bottom sediments in lakes using hydroacoustic methods and comparison with laboratory measurements. Water Res. 45, 4399–4408.

Angel, J.R., Kunkel, K.E., 2010. The response of Great Lakes water levels to future climate scenarios with an emphasis on Lake Michigan–Huron. J. Great Lakes Res. 36, 51–58.

APHA, 1998. Standard Methods for the Examination of Water and Wastewater, 20th edition. American Public Health Association, Washington, DC.

Barko, J.W., Hardin, D.G., Matthews, M.S., 1984. Interactive influences of light and temperature on the growth and morphology of submersed freshwater macrophytes. Technical Report A-84-3. U.S. Army Corps of Engineers, Waterways Experiment Station, Vicksburg, MS (24 pp.).

Barko, J.W., Gunnison, D., Carpenter, S.R., 1991. Sediment interactions with submersed macrophyte growth and community dynamics. Aquat. Bot. 41, 41–65.

Best, E.P.H., Teeter, A.M., Landwehr, K.J., James, W.F., 2008. Restoration option for potential persistence of submersed aquatic vegetation: combining ecological hydrodynamic and sediment transport modeling. Freshw. Biol. 53, 814–826.

BioSonics, 2007. User Guide, Visual Bottom Typer (VBT) 1.12 (With Depth Normalization). BioSonics, Inc., 4027 Leary Way NW, Seattle, WA.

BioSonics, 2010. User Guide, Visual Acquisition 6.0.1. BioSonics, Inc., 4027 Leary Way NW, Seattle, WA.

Bornett, G., Puijalon, S., 2011. Response of aquatic plants to abiotic factors: a review. Aquat. Sci. 73, 1–14.

Brady, V., Reschke, C., Breneman, D., Host, G., Johnson, L., 2010. 40th Avenue West Remediation to Restoration Project: Biological Survey Results. Natural Resources Research Institute, University of Minnesota, Duluth (Contracted by the United States Fish and Wildlife Service Cooperative Agreement 30181AJ68. NRRI/TR-2012/24).

Breiman, L., Friedman, J.H., Olsen, R.A., Stone, C.G., 1984. Classification and Regression Trees. Wadsworth International Group, Belmont, CA.

Burrough, P.A., McDonell, R.A., 1998. Principles of Geographical Information Systems. Oxford University Press, NY (190 pp.).

Carpenter, S.R., Lodge, D.M., 1986. Effects of submersed macrophytes on ecosystem processes. Aquat. Bot. 26, 341–370.

Carter, V., Paschal Jr., I.J., Bartow, N., 1985. Distribution and abundance of submersed aquatic vegetation in the tidal Potomac River and Estuary, Maryland and Virginia, May 1978 to November 1981—a water quality study of the tidal Potomac River and Estuary. U. S. Geol. Surv. Water Supply Pap. 2234A (46 pp.).

Catling, P.M., Spicer, K.W., Biernacki, M., Lovett-Doust, J., 1994. The biology Canadian weeds. 103. *Vallisneria americana* Michx. Can. J. Plant Sci. 74, 883–897.

Cerco, C.F., Moore, K., 2001. System-wide submerged aquatic vegetation model for Chesapeake Bay. Estuaries 24, 522–534.

Christiansen, C., Christoffersen, H., Dalsgaard, J., Nornberg, P., 1981. Coastal and near-shore changes correlated with die-back in eelgrass (*Zostera marina* L.). Sediment. Geol. 28, 163–173.

Croft, M.V., Chow-Fraser, P., 2007. Use and development of the Wetland Macrophyte Index to detect water quality impairment in fish habitat of Great Lakes coastal marshes. J. Great Lakes Res. 33, 172–197.

Cvetkovic, M., Wei, A., Chow-Fraser, P., 2010. Relative importance of macrophyte community versus water quality variables for predicting fish assemblages in coastal wetlands of the Laurentian Great Lakes. J. Great Lakes Res. 36, 64–73.

Czuba, C.R., Fallon, J.D., Kessler, E.W., 2012. Floods of June 2012 in Northeastern Minnesota. U.S. Geological Survey, Scientific Investigations Report 2012–5283. (42 pp. http://pubs.usgs.gov/sir/2012/5283/sir2012-5283.pdf. Accessed 7 August 2013).

Depew, D.C., Houben, A.J., Ozersky, T., Hecky, R.E., Guildform, S.J., 2010. Submerged aquatic vegetation in Cook's Bay, Lake Simcoe: assessment of changes in response to increase water transparency. J. Great Lakes Res. 37, 72–82.

DeVore, P.W., 1978. Fisheries Resources of the Superior–Duluth Estuarine Waters. Center for Lake Superior Environmental Studies, Superior, WI.

Duarte, C.M., Kalff, J., 1986. Littoral slope as a predictor of the maximum biomass of submerged macrophyte communities. Limnol. Oceanogr. 31, 1072–1080.

Duarte, C.M., Kalff, J., 1990. Patterns in the submerged macrophyte biomass of lakes and the importance of scale of analysis in the interpretation. Can. J. Fish. Aquat. Sci. 47, 357–363.

Gönen, M., 2006. Receiver Operating Characteristics (ROC) Curves. Memorial Sloan-Kettering Cancer Center, 1275 York Avenue, New York, NY 10021 (http://www.mskcc.org/mskcc/html/3185.cfm. Accessed 7 August 2013).

Havens, K.E., Harwell, M.C., Brady, M.A., Sharfstein, B., East, T.L., Rodusky, A.J., Anson, D., Maki, R.P., 2002. Large-scale mapping and predictive modeling of submerged aquatic vegetation in a shallow eutrophic lake. Sci. World J. 2, 649–965.

Host, G., Reschke, C., Brady, V., Breneman, D., Dumke, J., Niemi, G., Austin, J., James, M., Johnson, L., 2012. 21st Avenue West Remediation to Restoration Project: Biological Survey and Hydrodynamic Modeling. Natural Resources Research Institute, University of Minnesota, Duluth (Contracted by the United States Fish and Wildlife Service Cooperative Agreement F11AC00517).

Hudon, C., Lalonde, S., Gagnon, P., 2000. Ranking the effects of site exposure, plant growth form, water depth, and transparency on aquatic plant biomass. Can. J. Fish. Aquat. Sci. 57, 31–42.

Hunt, G.S., 1963. Wild celery in the lower Detroit River. Ecology 44, 360–370.

International Upper Great Lakes Study (IUGLS), 2012. Lake Superior Regulation: Addressing Uncertainty in Upper Great Lakes Water Levels. (http://www.ijc.org/iuglsreport/wp-content/report-pdfs/Lake_Superior_Regulation_Full_Report.pdf. Accessed 7 August 2013).

Jude, D.J., Pappas, J., 1992. Fish utilization of Great Lakes coastal wetlands. J. Great Lakes Res. 18, 651–672.

Kahn, J.R., Kemp, W.M., 1985. Economic losses associated with the degradation of an ecosystem: the case of submerged aquatic vegetation in Chesapeake Bay. J. Environ. Econ. Manag. 12, 246–263.

Kaul, R.B., 1978. Morphology of germination and establishment of aquatic seedlings in Alismataceae and Hydrocharitaceae. Aquat. Bot. 5, 139–147.

Keddy, P.A., 1982. Quantifying within-lake gradients of wave energy: interrelationships of wave energy, substrate particle size and shoreline plants in Axe Lake, Ontario. Aquat. Bot. 14, 41–58.

Knapton, R.W., Petrie, S.A., 1999. Changes in distribution and abundance of submerged macrophytes in the Inner Bay at Long Point, Lake Erie: implications for foraging waterfowl. J. Great Lakes Res. 25, 783–798.

Koch, E.W., 2001. Beyond light: physical, geological, and geochemical parameters as possible submersed aquatic vegetation habitat requirements. Estuaries 24, 1–17.

Korschgen, C.E., Green, W.L., 1988. American wild celery *Vallisneria americana*: ecological considerations for restoration. U.S. Fish and Wildlife Service, Fish and Wildlife Technical Report 19. Northern Prairie Wildlife Research Center Online, Jamestown, ND (http://www.npwrc.usgs.gov/resource/plants/wildcel/index.htm Version 16JUL97). Accessed 7 August 2013).

Korschgen, C.E., Green, W.L., Kenow, K.P., 1997. Effects of irradiance on growth and winter bud production by *Vallisneria americana* and consequences to its abundance and distribution. Aquat. Bot. 58, 1–9.

Kreiling, R.M., Yin, Y., Gerber, T., 2007. Abiotic influences on the biomass of *Vallisneria americana* Michx. in the Upper Mississippi River. River Res. Appl. 23, 343–349.

Krieger, K.A., 1992. The ecology of invertebrates in Great Lakes coastal wetlands: current knowledge and research needs. J. Great Lakes Res. 18, 634–650.

Larson, J.H., Trebitz, A.S., Steinman, A.D., Wiley, M.J., Mazur, M.C., Pebbles, V., Braun, H.A., Seelbach, P.W., 2013. Great Lakes Rivermouth Ecosystems: Scientific Synthesis and Management Implications. http://dx.doi.org/10.1016/j.jglr.2013.06.002 (Accessed 7 August 2013).

Legendre, P., 1993. Spatial autocorrelation: trouble or new paradigm? Ecology 74, 1659–1673.

Louvet-Doust, J., LaPorte, G., 1991. Population sex ratios, population mixtures and fecundity in a dioecious macrophyte, *Vallisneria americana*. J. Ecol. 79, 477–489.

Madsen, J.D., Chambers, P.A., James, W.F., Koch, E.W., Westlake, D.F., 2001. The interactions between water movement, sediment dynamics, and submersed macrophytes. Hydrobiologia 444, 71–84.

Magner, J., Brooks, K., 2008. Predicting stream channel erosion in the lacustrine core of the upper Nemadji River, Minnesota (USA) using stream geomorphology metrics. Environ. Geol. 54, 1423–1434.

Minnesota Department of Natural Resources (MNDNR), 2012. Minnesota's Sensitive Lakeshore Identification Manual: A Conservation Strategy for Minnesota Lakeshores (Version 3). Division of Ecological and Water Resources, Minnesota Department of Natural Resources (87 pp. http://files.dnr.state.mn.us/eco/sli/sens_lakeshore_manual.pdf. Accessed 7 August 2013).

Narumalani, S., Jensen, J.R., Althausen, J.D., Burkhalter, S., Mackey Jr., H.E., 1997. Aquatic macrophyte modeling using GIS and logistic multiple regression. Photogramm. Eng. Remote Sens. 63, 41–49.

Ojakangas, R.W., Matsch, C.L., 1982. Minnesota's Geology. University of Minnesota Press, Minneapolis, MN.

Orth, R.J., Williams, M.R., Marion, S.R., Wilcox, D.J., Carruthers, T.J.B., Moore, K.A., Kemp, M., Dennison, W.C., Rybicki, N., Bergstrom, P., Batiuk, R.A., 2010. Long-term trends in submerged aquatic vegetation (SAV) in Chesapeake Bay, USA, related to water quality. Estuar. Coasts 33, 1144–1163.

Prince, H.P., Padding, P.I., Knapton, R.W., 1992. Waterfowl use of the Laurentian Great Lakes. J. Great Lakes Res. 18, 673–699.

Randall, R.G., Minns, C.K., Cairns, V.W., Moore, J.E., 1996. The relationship between an index of fish production and submerged macrophytes and other habitat features at three littoral areas in the Great Lakes. Can. J. Fish. Aquat. Sci. 53, 35–44.

Reschke, C., Host, G., 2013. Are chemicals of emerging concern (CECs) limiting growth of aquatic plants in the St. Louis River Estuary? Presentation at Annual Meeting of Society of Wetland Scientists, Duluth, MN, June 3, 2013 (http://sws2013.conferencespot.org Accessed 7 August 2013).

Rodusky, A.J., Sharfstein, B., East, T.L., Maki, R.P., 2005. A comparison of three methods to collect submerged aquatic vegetation in a shallow lake. Environ. Monit. Assess. 110, 87–97.

Rohweder, J., Rogala, T., Johnson, B.L., Andersons, D., Clark, S., Chamberlin, F., Runyon, K., 2008. Application of wind fetch and wave models for habitat rehabilitation and enhancement projects. U.S. Geological Survey, Open-File Report 2008-120.

Sabol, B.M., Kannenberg, J., Skogerboe, J.G., 2009. Integrating acoustic mapping into operational aquatic plant management: a case study in Wisconsin. J. Aquat. Plant Manage. 47, 44–52.

Sierszen, M.E., Morrice, J.A., Trebitz, A.S., Hoffman, J.C., 2012. A review of selected ecosystem services provided by coastal wetlands of the Laurentian Great Lakes. Aquat. Ecosyst. Health Manage. 15, 92–106.

Skubinna, J.P., Coon, T.G., Batterson, T.R., 1995. Increased abundance and depth of submersed macrophytes in response to decreased turbidity in Saginaw Bay, Lake Huron. J. Great Lakes Res. 21, 476–488.

Spence, D.H.N., 1982. The zonation of plants in freshwater lakes. Adv. Ecol. Res. 12, 27–125.

Spink, A., Rogers, S., 1996. The effects of a record flood on the aquatic vegetation of the Upper Mississippi River Systems: some preliminary findings. Hydrobiologia 340, 51–57.

St. Louis River Citizens Action Committee (SLRCAC), 2002. Lower St. Louis River Habitat Plan. The St. Louis River Alliance (http://www.stlouisriver.org/habitatplan2.html. Accessed 7 August 2013).

Stewart, R.M., McFarland, D.G., Ward, D.L., Martin, S.K., Barko, J.W., 1997. Flume study investigation of navigation-generated waves on submersed aquatic macrophytes. ENV Report 1, September 1997.Illinois Water System Navigation Study, Upper Mississippi River (62 pp.).

Titus, J.E., Adams, M.S., 1979. Comparative carbohydrate storage and utilization patterns in the submersed macrophytes, *Myriophyllum spicatum* and *Vallisneria americana*. Am. Midl. Nat. 102, 263–272.

Trebitz, A.S., Brazner, J.C., Cotter, A.M., Knuth, M.L., Morrice, J.A., Peterson, J.S., Sierszen, M.E., Thompson, J.A., Kelly, J.R., 2007. Water quality in Great Lakes coastal wetlands: basin-wide patterns and responses to an anthropogenic disturbance gradient. J. Great Lakes Res. 33, 67–85.

Valley, R.D., Drake, M.T., Anderson, C.S., 2005. Evaluation of alternative interpolation techniques for the mapping of remotely-sensed submersed vegetation abundance. Aquat. Bot. 81, 13–25.

Wigand, C., Wehr, J., Kimburg, K., Gorham, B., Longergan, S., Findlay, S., 2000. Effects of *Vallisneria americana* (L.) on community structure and ecosystem function in lake ecosystems. Hydrobiology 418, 137–146.

Wilkinson, L., 1998. Classification and Regression Trees. SYSTAT 10.0 Statistics, SPSS, Inc., Chicago, IL.

Wilson, S.D., Keddy, P.A., 1986. Species competitive ability and position along a natural stress/disturbance gradient. Ecology 67, 1236–1242.

Winfield, I.J., Onoufriou, C., O'Connell, M.J., Godlewska, M., Ward, R.M., Brown, A.F., Yallop, M.L., 2007. Assessment in two shallow lakes of a hydroacoustic system for surveying aquatic macrophytes. Hydrobiologia 584, 111–119.

Wolter, P.T., Johnston, C.A., Niemi, G.J., 2005. Mapping submergent aquatic vegetation in the US Great Lakes using Quickbird satellite data. Int. J. Remote. Sens. 26, 5255–5274.

Zhu, B., Fitzgerald, D.G., Hosking, S.B., Rudstam, L.G., Mayer, C.M., Mills, E.L., 2007. Quantification of historical changes of submerged aquatic vegetation cover in two bays of Lake Ontario with three complementary methods. J. Great Lakes Res. 33, 122–135.